https://doi.org/10.5194/egusphere-2026-3761
Preprint. Discussion started: 15 September 2026

A coupled cosmogenic-modelling approach to quantifying Holocene erosion of Ireland's hard-rock coastal cliffs

Gregor M. Rink[1,2], Gordon R. M. Bromley[1,2,3], Brenda L. Hall[3], Alan J. Hidy[4], Zuzanna M. Swirad[5]

[1]Geography, University of Galway, Galway, H91 TK33, Ireland
[2]Research Ireland Centre for Applied Geosciences (iCRAG), University College Dublin, Belfield, D04 C1P1, Ireland
[3]School of Earth & Climate Science and the Climate Change Institute, University of Maine, Orono, ME 04469-5790, United States of America
[4]Center for Accelerator Mass Spectrometry, Lawrence Livermore National Laboratory, Livermore, CA 94550, United States of America
[5]Institute of Geophysics, Polish Academy of Sciences, Warsaw, Poland

Correspondence to: Gregor M. Rink (g.rink1@universityofgalway.ie)

Abstract

Hard rock cliffs and shore platform are a key feature of the coastal environments in Ireland. Being highly influenced by marine driven erosion, the relationship between changes in relative sea level (RSL) and cliff retreat rates are of major interest when analysing coastal evolution. At the western coast of Ireland, the rates of RSL rise in the Holocene has varied and some locations experienced marine driven erosion earlier than others. Therefore, for understanding coastal hard-rock erosion and the influences of long-term changes, such as RSL changes, studying multiple at locations is crucial.

In this study, we investigated cliff erosion rates on millennial scales at two locations on the western Irish coast – Muckros Head and Ballard Bay – using cosmogenic beryllium-10 concentrations. Our findings indicate that the shore platforms at both locations were formed entirely during the Holocene, and that each site has experienced a long-term deceleration in cliff retreat, reflecting declining rates of RSL rise. The cliff retreat rate decelerated from 14 to 1 mm yr^{-1} at Muckros Head within the past ~9500 yrs, and from 25 to 5 mm yr^{-1} at Ballard Bay over the last ~5000 yrs. The best-fit models suggest shore platform widening at Muckros Head and steady-state erosion at Ballard Bay. Whereas the pronounced deceleration in cliff retreat observed at Muckros Head, relative to Ballard

https://doi.org/10.5194/egusphere-2026-3761
Preprint. Discussion started: 15 September 2026

Bay, is explained by the elevated early-Holocene RSL at the former, differences in contemporary retreat rates between our sites likely reflect contrasting geomorphological and geological conditions and marine environments.

1 Introduction

Cliffs and shore platforms constitute elementary features of rocky coasts worldwide, and growing human pressure on coastal zones underlines the importance of quantifying erosion rates of cliffs and platforms and driving mechanisms (Trenhaile, 2008; Prémaillon et al., 2018; Young and Carilli, 2019; Cosby et al., 2024). Any analysis of rocky coast erosion should incorporate multiple parameters, reflecting the diverse environmental settings. Lithology, tidal range, wave energy, storminess and relative sea level (RSL) variability are among the primary parameters governing cliff retreat (e.g., Trenhaile, 2000, 2008; Hurst et al., 2017; Prémaillon et al., 2018); the vertical erosion of shore platforms, known as down-wearing, is also depended on other factors, such as tidal cycles of wetting and drying, bioerosion and clast abrasion (Kennedy et al., 2014; Cullen and Bourke, 2018; Clow et al., 2023).

In recent decades, numerous methods have been developed to investigate rocky coast erosion and identify driving processes at a range of spatio-temporal scales. Shore platform down-wearing is measured predominantly with micro erosion meters (MEMs) (e.g., Stephenson, 2000; Stephenson et al., 2010; Furlani and Cucchi, 2013; Trenhaile and Porter, 2018), while cliff retreat rates are typically derived from temporal changes in shoreline configurations established via (i) orthophotography and maps (e.g., Dornbusch et al., 2006, 2008; Ruggiero et al., 2013) and (ii) 3D models of the cliff surface generated from Structure-from-Motion (SfM), Terrestrial Laser Scanning (TLS) and/or Light Detection and Ranging (LiDAR) surveys (Williams et al., 2019; Gómez-Pazo et al., 2021; Swirad and Young, 2022; Rink et al., 2024). Cartographical sources can date back to mid-19th Century in some locations, but high-precision methods (SfM, TLS, LiDAR) have been widely used only for the last 20-30 years (Ruggiero et al., 2013; Colomina and Molina, 2014).

For investigating cliff retreat on longer (e.g., Holocene) timescales, analysis of cosmogenic beryllium-10 (^{10}Be) concentrations has become an increasingly viable tool, with multiple applications over the past decade (e.g., Regard et al., 2012; Hurst et al., 2016; Swirad et al., 2020; Shadrick et al., 2021; Jeong et al., 2024). At any point on Earth's surface, *in situ* beryllium-10 (^{10}Be) accumulates over time in the lattices of common minerals such as quartz; concurrently, surface erosion serves to remove accumulated ^{10}Be (Lal, 1991; Gosse and Phillips, 2001). While most of the production occurs close to the rock surface via spallation from high-energy neutrons (Balco, 2017; Gosse and Phillips, 2001), production via fast muons becomes increasingly important with depth (Balco,

https://doi.org/10.5194/egusphere-2026-3761
Preprint. Discussion started: 15 September 2026

2017; Braucher et al., 2003). Isotope production depends both on global parameters, such as atmospheric shielding and latitudinal variations in the geomagnetic field, which are accounted for by scaling models, and on site-specific shielding factors (e.g., geological, environmental, geographical settings) and exposure time of the surface (Gosse and Phillips, 2001; Balco et al., 2008). In tidal zones, ^{10}Be production is further impacted by the shielding effect of water due to changes in relative sea level (RSL) and tidal coverage, and also beach sediment cover (Hurst et al., 2017; Regard et al., 2012; Shadrick et al., 2021; Swirad et al., 2020), thus complicating the estimation of cliff-retreat rates via surface-exposure ages alone (Regard et al., 2012; Rogers et al., 2012). Therefore, a different approach is to compare modelled and measured ^{10}Be concentrations in samples collected from adjacent shore platforms (Choi et al., 2012; Regard et al., 2012; Hurst et al., 2016; Swirad et al., 2020; Shadrick et al., 2022; Jeong et al., 2024).

Previous studies have applied various approaches to investigate the relationship(s) between platform down-wearing and cliff retreat rates, and their respective influences on ^{10}Be-concentration. In one simplified approach the cliff retreat rate is taken as being independent from shore platform erosion, which is assumed to be negligible (Choi et al., 2012; Swirad et al., 2020; Jeong et al., 2024). Alternatively, for studies in which shore platform down-wearing and cliff retreat are coupled, one might assume a proportional relationship between the two, whereby the shape of the platform profile does not change with time (Regard et al., 2012; Hurst et al., 2016; Swirad et al., 2020; Jeong et al., 2024). In cases where a shore platform's seaward edge maintains a laterally and vertically stable position below the wave base, marine-driven erosion (e.g., waves, tides, bioagents) might cause widening and flattening of the shore platform in concert with cliff retreat (Flemming, 1965; Hurst et al., 2017; Swirad et al., 2020). Superimposed upon long-term pattern of down-wearing, the detachment of blocks by waves also exerts a strong influence on shore platform erosion and profile and, ultimately, upon cliff retreat, and thus must be considered in evaluations of structurally-controlled rocky coast evolution (Hurst et al., 2017; Swirad et al., 2020).
In this study, we apply the geometric model of Swirad et al. (2020) and Jeong et al. (2024) to investigate average long-term rates of cliff retreat in two high-energy environments on the west coast of Ireland. The model incorporates recent platform shape, RSL variabilities, and tidal distributions to compute plausible cliff retreat and shore platform down-wearing scenarios for a predefined recent cliff retreat rate. We then compare these scenarios to measured ^{10}Be concentrations in rock samples collected from the shore platform surface. By investigating two contrasting sites, this study aims to establish (i) whether the target shore platforms are products of ongoing Holocene erosion or relics from earlier sea-level high stands, and (ii) the influences of local parameters (e.g., lithology, RSL, wave climate) on long-term cliff retreat rates.

https://doi.org/10.5194/egusphere-2026-3761
Preprint. Discussion started: 15 September 2026

2 Study sites

2.1 Regional overview

Our investigation focuses on two sites on the west coast of Ireland: Muckros Head (54.61° N, 8.59° W) in County Donegal and Ballard Bay (52.74° N, 9.61° W) in County Clare (Figure 1). While both sites experience a strong oceanic climate characterised by high precipitation and prevailing SW–W winds (Cooper et al., 2004; Lozano et al., 2004; Peel et al., 2007), Muckros Head experiences slightly wetter (1200–1400 mm yr^{-1}) and colder (9–10 °C mean annual temperature) conditions than Ballard Bay (1000–1200 mm yr^{-1} and 10-11 °C) (Walsh, 2012). Both settings are subject to the Atlantic wave regimes; significant wave heights on Ireland's west coast are typically 3–3.5 m but can surpass 5 m during winter months (Gallagher et al., 2013, 2014; Tiron et al., 2015) and 10 m during storms (O'Brien et al., 2018).

https://doi.org/10.5194/egusphere-2026-3761
Preprint. Discussion started: 15 September 2026

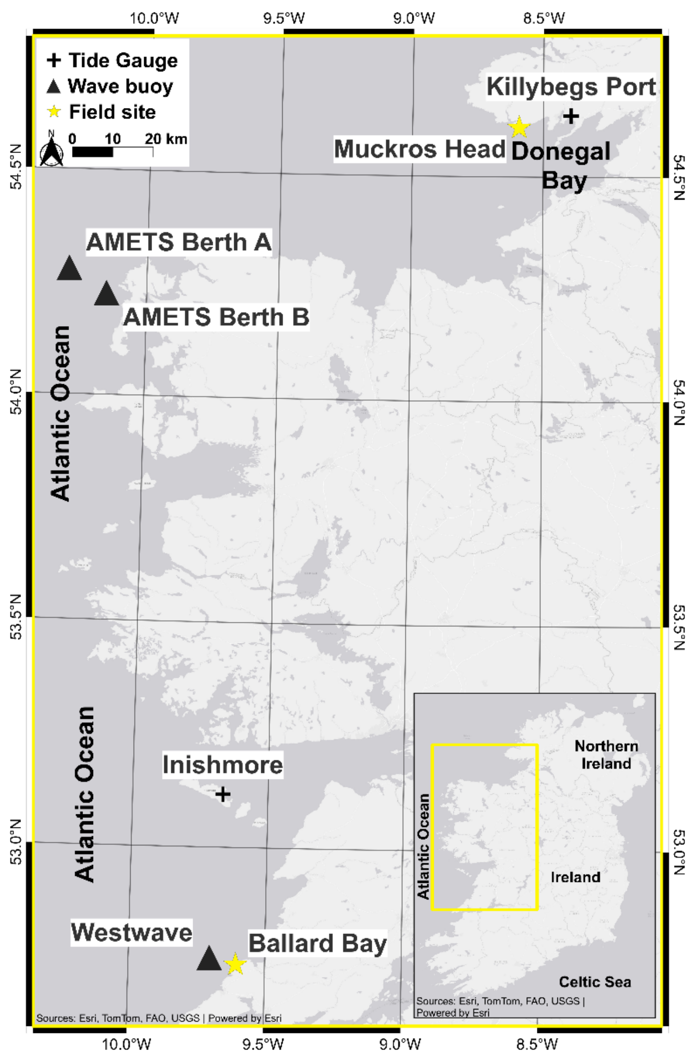

Figure 1: The two west coast study sites, Muckros Head and Ballard Bay (yellow stars), represent contrasting geologic, climatic, and marine settings. Muckros Head is a peninsula situated on the northern shore of Donegal Bay, ~13 km SW of Killybegs; Ballard Bay on the coast of County Clare is located ~40 km south of Inishmore. Background and inset map derived from ESRI Gray (light) (Sources: Esri, TomTom, FAO, USGS | Powered by Esri).

2.2 Muckros Head

The Muckros Head peninsula in County Donegal (54.609° N, 8.593° W) is situated on the northern shore of outer Donegal Bay. With its broad (~50 km wide) mouth opening onto the North Atlantic, Donegal Bay affords minimal protection against oceanic wave energy and weather systems, especially for the bay's northern coastline where Muckros Head is located. Geologically, Muckros Head is underlain by coarse-grained, carbonate-rich

https://doi.org/10.5194/egusphere-2026-3761
Preprint. Discussion started: 15 September 2026

Carboniferous sandstone. Our study site on the peninsula's north-western aspect exhibits an ~80 m-wide, gently sloping (1.05°) shore platform (Graham et al., 2014) (Figure 2). Bounded on its seaward edge by a sub-tidal cliff, the shore platform is a Type-B feature according to the scheme of Sunamura (1992). Inland of the shore platform, a series of 0.5–1 m-high terraces together form a stepped cliff with a total relief of ~10 m (Figure 2). The peninsula experiences meso-tidal ranges between 2 and 4 m (Minogue et al., 2020), causing regular inundation of the shore platform.

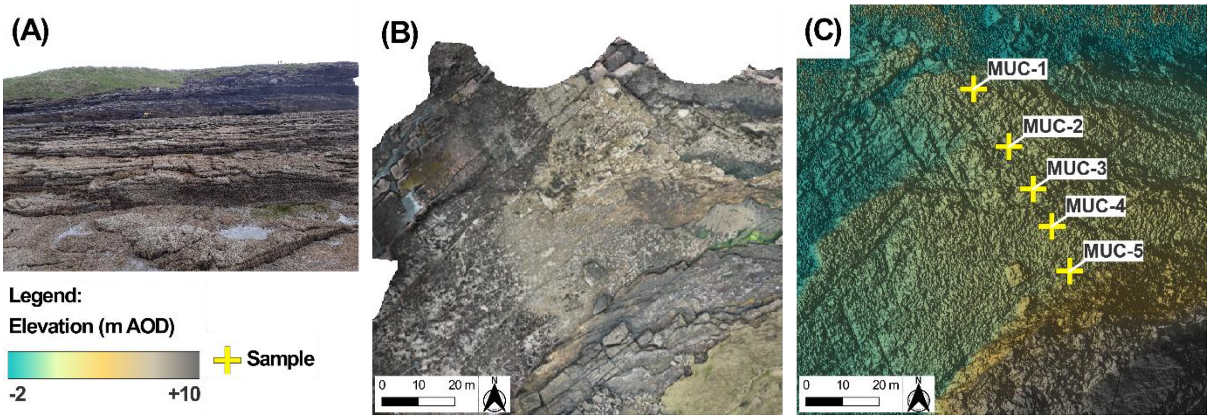

Figure 2: The shore platform and cliff at Muckros Head: (A) south-eastward view of the upper shore platform, lower terraces and cliff face, as seen from the outer platform; (B) orthoimage of the cliff line and shore platform; (C) Digital surface model of the same area as B with the ^{10}Be sample transect marked by yellow crosses and sample IDs. Elevations are given as metres above ordnance datum Malin Head.

The Muckros Sandstone Formation was deposited in an early Carboniferous shelf environment and is part of the Largymore Syncline, which extends between Muckros Head and Fintragh Bay (Davis et al., 2012; Graham et al., 2014). At the base of the formation is exposed a medium-to-coarse-grained calcareous sandstone, some layers of which contain occasional nodules and quartz pebbles. Overlying these basal rocks are finer-grained, frequently cross-bedded oolitic-sandy limestones, capped by micritic limestone (Graham et al., 2014). Most of these layers include fossils and bioturbation. Graham et al. (2014) interpreted the Muckros formation as representing a shallow, inshore, tidal marine high-energy environment with bipolar currents, and attributed that setting to regional shoreline transgression driven by either tectonic uplift or sea-level lowering (Graham et al., 2014). During Quaternary glaciations, Muckros Head and the surrounding area were inundated repeatedly by ice sheets; the most recent deglaciation occurring approximately 16,000 years ago (Ballantyne et al., 2007), but marine driven erosion at Muckros Head did not commence until eustatic sea level rise caught up with glacio-isostatic rebound during

https://doi.org/10.5194/egusphere-2026-3761
Preprint. Discussion started: 15 September 2026

the mid-Holocene (Shaw and Carter, 1994). The modern cliff and shore platform both exhibit evidence of karstification.

2.3 Ballard Bay

Approximately 220 km south-west of Muckros Head, Ballard Bay (52.740° N, 9.607° W) is a small (< 1 km^2) west-facing embayment located between the towns of Kilkee and Doonbeg in County Clare. Waves enter Ballard Bad primarily from the W–SW, with annual mean significant wave heights of 3–4 m(Gallagher et al., 2013), while semi-diurnal tides exhibit an average range of 4.5 m (Cullen and Bourke, 2018). Ballard Bay features a 1 km long and ~20 m high cliff, fronted by a gently sloping (2°–5°) shore platform with a maximum width of ~200 m (Figure 3). As at Muckros Head, the prominent sub-tidal cliff bounding the seaward edge of the Ballard Bay shore platform conforms with the Type-B classification of Sunamura (1992). Reflecting localised variations in the gradient and elevation of the platform, the high-water line during normal tidal ranges lies within 30–50 m distance of the base of the cliff. Nevertheless, active removal of rockfall debris indicates that waves regularly reach the cliff base (Cullen and Bourke, 2018).

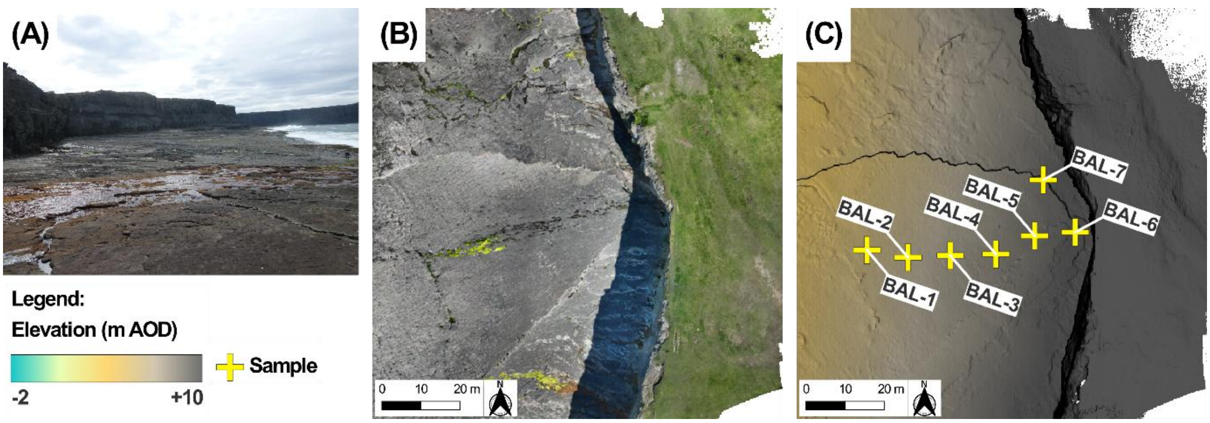

Figure 3: The shore platform and cliff at Ballard Bay: (A) southward view from the north end of the shore platform; (B) orthoimage of the cliff and shore platform, showing the terraces of the cliff and the shore platform; (C) Digital surface model of the shore platform and cliff, along with the ^{10}Be sample transect. Elevations are given as metres above ordnance datum Malin Head.

Ballard Bay is underlain by sandstones and siltstones deposited in the Clare Basin during mid-Carboniferous (~331–315 Ma) cycles of marine transgression and regression (Collinson et al., 1991; Pointon et al., 2012; Best et al., 2016). Local lithologies reveal terrestrial, deltaic, and deeper marine facies that are known collectively as the Tullig and Kilkee cyclothems (Collinson et al., 1991; Pointon et al., 2012; Best et al., 2016); the top of the

https://doi.org/10.5194/egusphere-2026-3761
Preprint. Discussion started: 15 September 2026

Tullig cyclothem forms the shore platform at our site, while the cliff face comprises the basal unit of the Kilkee cyclothem (Collinson et al., 1991; Cullen and Bourke, 2018; Nauton-Fourteu et al., 2020).

As in Donegal, the Clare coast was glaciated repeatedly during the Quaternary (Clark et al., 2022), with the most recent ice sheet vacating this region no later than 17,000 years ago (Bromley et al., 2026). According to Kuchar et al. (2012) and Shennan et al. (2018), glacio-isostatic adjustment over the last 5000 years has resulted in a relative sea-level rise of ~5 m. In their analysis of modern erosion processes, Cullen and Bourke (2018) analysed the impact of recent platform abrasion during storms by measuring the area and volume of stretch-and-percussion marks on the platform surface. They estimated an annual volume loss of 67,808 cm^3 for the 0.4 km^2 study area (Cullen and Bourke, 2018), corresponding to a platform down-wearing rate of 0.17 $\mu m\ yr^{-1}$.

3 Methods

3.1 Digital surface models and topographic profiles

As for most sections of Ireland's west coast, high-resolution digital elevation data are not publicly available for Muckros Head and Ballard Bay. Therefore, we conducted uncrewed aerial vehicle (UAV) surveys of each site to generate digital surface models (DSMs) using Structure-from-Motion (SfM) photogrammetry, following the workflows detailed by Westoby et al. (2012), Swirad et al. (2019), and Jeong et al. (2024). First, we conducted UAV surveys using a DJI Mavic 3 Enterprise survey drone with an in-built camera with focal length of 12.29 mm. We collected a series of near-vertical (80°) photographs with a 75–80% overlap. We deployed temporary ground control points (GCPs) on each shore platform surface and collected GCP coordinates, referenced to meters above ordnance datum (m AOD) Malin Head, using a Trimble GNSS to georeference the UAV data. DSMs were created from the UAV imagery and GNNS data using Agisoft Metashape (Version 1.5.5 9097) (Agisoft LCC, 2019). We used MATLAB to downscale the DSM to 0.5 m resolution and computed topographic profiles for each ^{10}Be transect via TopoToolbox (Version 2.3.1) (Schwanghart and Kuhn, 2010; Schwanghart and Scherler, 2014). Downscaling reduces the influence on the topographic profiles of any noise and artefacts generated during the DSM computing process. In addition to the topographic profiles, we also computed simplified profiles using linear least-squares regression lines along each topographic profile (Swirad et al., 2020; Jeong et al., 2024).

3.2 Cosmogenic ^{10}Be field methods

We collected rock samples for ^{10}Be measurement along longitudinal transects on each shore platform, following workflows established by Regard et al. (2012), Hurst et al. (2016), and Swirad et al. (2020) (Figure 2 and Figure

https://doi.org/10.5194/egusphere-2026-3761
Preprint. Discussion started: 15 September 2026

3). Specifically, we used a hammer and carbide-tipped chisel to remove the upper 5 cm of the rock surface. We sampled every ~30 m to ~50 m along horizontal transects oriented perpendicular to the cliff faces, from the intertidal to supratidal zone. We note that the Ballard Bay transect does not cover the entire ~100 m width of that platform, since the lowest ~40 m are within the high-energy wave swash zone and to access. The final transects comprised five samples at Muckros Head and seven samples at Ballard Bay. One sample of each transect was taken from a shielded location close to or at the cliff base (Muckros Head sample MUC-5 and Ballard Bay sample BAL-6) to estimate the concentration of background ^{10}Be in our samples (Hurst et al., 2016; Swirad et al., 2020; Jeong et al., 2024); this component reflects the sub-surface production of beryllium (primarily via deep muogenic production) prior to exposure of target rocks at the modern platform surface. Total sample mass depended on lithology, especially the estimated quartz content, and typically varied between ~2 kg and ~3.5 kg. To establish sample locations exactly, we used a high-accuracy (0.02–0.03 m) Trimble R8 PPK and R10 RTK Global Navigation and Satellite Systems (GNSS) (Figure 3). Sample elevations are given as m AOD Malin Head.

3.3 ^{10}Be laboratory methods

All samples were prepared for beryllium chemistry at the University of Galway. First, we used a wire brush to remove organic crusts, including barnacles and shells, after which samples were described (e.g., lithology, weathering state, organic covering, etc.), weighed, and measured with a calliper. Samples were then crushed and sieved to retrieve the 125–250 µm fraction, to account for the fine grain sizes that dominate both sites. To separate quartz grains, we first performed repeated sequential leaching in 6M HCl and NaOH, before removing heavier minerals via heavy liquid separation (2.8 g ml^{-1}). Quartz separates were then purified by successive leaching in weak (<2%) hydrofluoric acid (Kohl and Nishiizumi, 1992) and electromagnetic separation, using a Frantz magnetic separator. We modified the purification process for each site to address lithological differences in grain size and structure: the slightly coarser-grained sandstones from Muckros Head required less time in hydrofluoric acid (~three weeks total) to remove meteoric beryllium, whereas finer-grained siltstone samples from Ballard Bay required up to five weeks of successive leaching in ~1% hydrofluoric acid (Whitmore et al., 2022). Samples were then passed through the Frantz electromagnet a final time to remove any remaining impurities.

We dissolved 20–30 g of quartz, spiked with a custom-made phenakite ^9Be-carrier solution, in concentrated (50%) hydrofluoric acid, whereupon beryllium was isolated via ion chromatography following established protocols (e.g., Kohl and Nishiizumi, 1992; Ochs and Ivy-Ochs, 1997; Stone, 1998), converted to BeO via $Be(OH)_2$ precipitation with diluted NH_3 solution, mixed with niobium powder, and packed in cathodes for $^{10}Be/^9Be$ measurement. All Muckros Head samples and sample BAL-7 were processed and packed at the University of

https://doi.org/10.5194/egusphere-2026-3761
Preprint. Discussion started: 15 September 2026

Galway, while all Ballard Bay samples (except BAL-7) were processed at the University of Maine Cosmogenic Isotope Lab. Beryllium ratios of all samples and blanks were measured at the Center for Accelerator Mass Spectrometry (CAMS), Lawrence Livermore National Laboratory. All ratios of $^{10}Be/^{9}Be$ were measured against NIST-traceable standard 1-5-4 (aka 07KNSTD3110) from (Nishiizumi et al., 2007) with a nominal value of $2.851 \cdot 10^{-12}$.

3.4 Modelling shore platform evolution and cliff retreat rates

We simulated ^{10}Be concentrations along the two shore platform transects, using version 2.0 (Swirad, 2025) of the shore platform geometry-sensitive inverse model developed by Swirad et al. (2020).This approach makes the following assumptions: (1) cliff morphology has not changed over time; (2) shore platforms have not experienced periods of reburial (e.g., by beach material) since their original exposure; and (3) tidal regime have remained quasi-stable over the period of exposure (Swirad et al., 2020; Jeong et al., 2024). We employed a combination of regional modelled RSL data from Kuchar et al. (2012) and Shennan et al. (2018), and local RSL data from South Clare (Devoy et al., 1996) and West Donegal (Smith and Pilcher, 1973) (Table 1). Since the shore platform and cliff have likely been formed only during the past few thousand years, a period considerably shorter than the 1.4 Myr half-life of ^{10}Be, incorporating decay is not necessary for our study(Regard et al., 2012). Based on the three assumptions defined above, the concentration of ^{10}Be [^{10}Be] along a shore platform topographic profile can be calculated according to Eq. (1) (Swirad et al., 2020):

$$[^{10}Be] = P * t_{exp} * S_{topo} * S_w * S_{gm} * S_{er} \quad (1)$$

where P is the production rate of ^{10}Be at an unshielded surface at sea level. For this study, we employed the Rannoch Moor mid-point production rate of 3.912 ± 0.11 atoms g^{-1} yr^{-1} (Putnam et al., 2019), scaled with time-invariant ('St') scaling method of Lal (1991) and Stone (2000). Exposure time in years is represented by t_{exp}. The model further includes two shielding factors - the topographic shielding, S_{topo}, and the water shielding, S_w, as well as the geomagnetic scalar, S_{gm}, and the platform erosion scalar, S_{er}. In shore platform settings, S_{topo} takes into account cliff height, cliff inclination and subtended azimuth (cliff line shape), and distance to the cliff (Dunne et al., 1999; Swirad et al., 2020). The factor S_w depends on both changes in RSL and in tidal regime; the latter incorporates the distribution of tidal duration and was estimated from data from the nearest tidal/sea level buoy (Figure 1) (Hurst et al., 2017; Swirad et al., 2020). S_{gm} is modelled after Lifton et al. (2014), while S_{er} reflects platform down-wearing, under the premise that rocks forming the current platform surface experienced lower

https://doi.org/10.5194/egusphere-2026-3761
Preprint. Discussion started: 15 September 2026

accumulation values prior to exposure. To accommodate variable erosion scenarios, therefore, each simulation incorporates a run-specific S_{er} (Swirad et al., 2020). A detailed overview of applied site specific model parameters is given in Table 1.

Table 1. Overview of the cliff parameters and RSL anchor points for modelling cliff retreat rates at Muckros Head and Ballard Bay.

Field site	Cliff height (m)	Cliff inclination (°)	Tidal range (m)	RSL time (yr BP)	RSL (m)	RSL data source
Muckros Head	8	90	3.2	0 2079 4466 5974 9416	0 0 -0.09 -0.97 -2.82	(Smith and Pilcher, 1973; Kuchar et al., 2012; Shennan et al., 2018)
Ballard Bay	17	90	3.7	0 406 554 593 2274 5000	0 -0.15 -0.33 -0.3 -1.25 -5.00	(Devoy et al., 1996; Kuchar et al., 2012; Shennan et al., 2018)

To evaluate the effects of changing cliff retreat rates and shore platform erosion rates during the Holocene, we applied sets of decelerating, accelerating, and constant cliff retreat rates and combined them with three different platform erosion models. The 'zero platform erosion' model ignores shore platform down-wearing (Choi et al., 2012; Swirad et al., 2020), whereas the 'steady-state' model assumes a proportional relationship between cliff retreat and platform down-wearing (Trenhaile, 1974; Regard et al., 2012), and also incorporates fluctuations in sea level (Swirad et al., 2020). The 'platform widening' model assumes a stable seaward edge of the topographic profile, which results in widening and flattening of the shore platform during cliff retreat (Flemming, 1965; Hurst et al., 2017; Swirad et al., 2020). In this third model, we used a simplified profile to simulate erosion rates relative to changes in platform width and slope (Swirad et al., 2020; Jeong et al., 2024).

All three platform erosion models require as input a recent cliff retreat rate to serve as a boundary condition for deceleration and acceleration scenarios, and also as a starting value for steady-retreat scenarios, to which increasing values are applied for each model run (Swirad et al., 2019; Jeong et al., 2024). Since contemporary

https://doi.org/10.5194/egusphere-2026-3761
Preprint. Discussion started: 15 September 2026

cliff retreat rates are not available, we performed four runs incorporating a range of recent cliff-retreat rates: the first run applies a rate of 50 mm yr^{-1}, as used in the original model of Swirad et al. (2020); the second and third runs employ rates of 10 mm yr^{-1} and 5 mm yr^{-1}, respectively, to investigate whether the recent cliff retreat rates are more likely to be within scales low cm yr^{-1} or high mm yr^{-1}. The fourth run was performed with 1 mm yr^{-1} to test recent cliff retreat rates of low mm yr^{-1} scales. For each recent cliff retreat rates, we tested 60 scenarios for various decelerating, accelerating and steady cliff retreat behaviour. The scenarios contained 20 steady retreat scenarios vary from the assumed recent values to be 1-20 times higher and 20 deceleration and acceleration scenarios, assuming a 1-20 higher/lower starting cliff retreat rate of than the recent.

Ultimately, cliff retreat and shore platform evolution are estimated by comparing the modelled ^{10}Be concentrations with those, measured from the transect samples (see Section 4.3). For this, we corrected all measured ^{10}Be concentrations for sample thickness (Balco et al., 2008) and any background ('inherited') nuclide component (Regard et al., 2012; Hurst et al., 2016; Swirad et al., 2019; Shadrick et al., 2022). For the comparison, we calculated the mean square difference (*MSD*) between corrected measured (S_i) and modelled (M_i) ^{10}Be concentration (Eq. (2)) (Swirad, 2025).

$$MSD = (M_i - S_i)^2 \tag{2}$$

The smallest MSD gives the optimal combination of shore platform erosion model and cliff retreat scenario (Swirad, 2025). Based on the MSD, the model uncertainties for ^{10}Be concentrations and cliff retreat rates are derived from the normalized root mean square difference (*NRMSD*), using the range between highest and lowest measured ^{10}Be-concentration for normalization. A common benchmark for reliable output from this model is a NRMSD < 0.2 (Swirad et al., 2020; Jeong et al., 2024, 2026).

3.5 Significant wave height and wave direction

Time-averaged significant wave height (Hs) and wave direction data are derived from three wave buoys operated by the Marine Institute (DigitalOcean.ie, 2025). Two installations – the AMETS Beth A and AMETS Beth B wave buoys – are situated off the north-west coast of County Mayo, approximately 100 km SW of Muckros Head. A third installation – the Westwave wave buoy – is located only 7 km NW of Ballard Bay (Figure 1). Owing to variations in data availability, analysis periods differ among the three stations: AMETS Beth A wave buoy spans the period 19/05/2019–22/07/2025; AMETS Beth B wave buoy spans the period 14/05/2015–22/07/2025; and Westwave wave buoy spans the period 15/05/2015–37/03/2019) (DigitalOcean.ie, 2025).

4 Results

4.1 Topography

At both sites, the DSM and cross shore profile reveal sloping shore platforms, with cliff bases are ~2.5 m (Muckros Head) and ~10 m (Ballard Bay) above 0 m AOD. At Muckros Head, the shore platform surface is much rougher and consist of more steps (Figure 2, Figure 4) than at Ballard Bay, which exhibits a relatively smooth shore platform profile (Figure 3, Figure 4). The total spatial errors of the computed DSMs are 1.1 cm for Muckros Head and 10.8 cm for Ballard Bay. The final DSMs have a pixel resolution of 0.0299 m (Muckros Head) and 0.024 m (Ballard Bay) with maximal point densities of 112 points m^{-2} for Muckros Head and 173 points m^{-2} for Ballard Bay (Table 2).

Table 2: Summary of the SfM surveys at Muckros Head and Ballard Bay.

Field site	Images total	Images aligned	GCP	Horizontal error (cm)	Vertical error (cm)	Total spatial error (cm)	Resolution (m)	Point density (points m^{-2})
Muckros Head	1497	1495	5	1.0563	0.2035	1.0757	0.0299	112
Ballard Bay	280	280	5	10.1423	3.8257	10.8399	0.0240	173

4.2 Measured cosmogenic ^{10}Be concentrations

The 61 m Muckros Head transect extends from the base of the lowest cliff terrace almost to the outer platform edge (Figure 2), and traverses a relatively stepped shore platform surface, which exhibits clear evidence for karstification, such as dissolution hollows and pedestals. In contrast, the Ballard Bay transect extends ~57 m across a comparatively smooth platform surface that, with the exception of samples BAL-6 and BAL-7, comprises a single bedding plane (Figure 3).

At both sites, the measured concentrations of cosmogenic ^{10}Be increase with distance from the cliff base and attain maximum values on the outer shore platform (Figure 4); neither transect exhibits samples with anomalously high ^{10}Be concentrations. At Muckros Head, the concentration of ^{10}Be in the shielded sample MUC-5, collected from the foot of the cliff, is 5886 ± 812 atoms g^{-1}. Corrected for this 'background' value and respective sample thicknesses, the remainder of the Muckros Head transect samples give ^{10}Be concentrations that range from 17,089 ± 1173 atoms g^{-1} (MUC-4) on the inner shore platform to 32,251 ± 1284 atoms g^{-1} (MUC-1) at the platform's seaward edge. Nonetheless, we note that sample MUC-2 exhibits a relatively low concentration (12,016 ± 1030 atoms g^{-1}) compared to the overall pattern (Table 3) and discuss plausible reasons for this deviation in section 5. At Ballard Bay, the shielded sample BAL-6 gives a background ^{10}Be concentration of 5521 ± 418 atoms g^{-1} (Table

https://doi.org/10.5194/egusphere-2026-3761
Preprint. Discussion started: 15 September 2026

3). Sample BAL-5 failed to yield sufficient current for a measurement and thus is excluded from further consideration. Consequently, we collected an additional sample (BAL-7) from ~15 m north of the transect line so as to complete the transect with a less problematic rock composition. Background- and thickness-corrected measurements from this transect range from 1679 ± 599 atoms g^{-1} (BAL-7) to 13,747 ± 759 atoms g^{-1}.

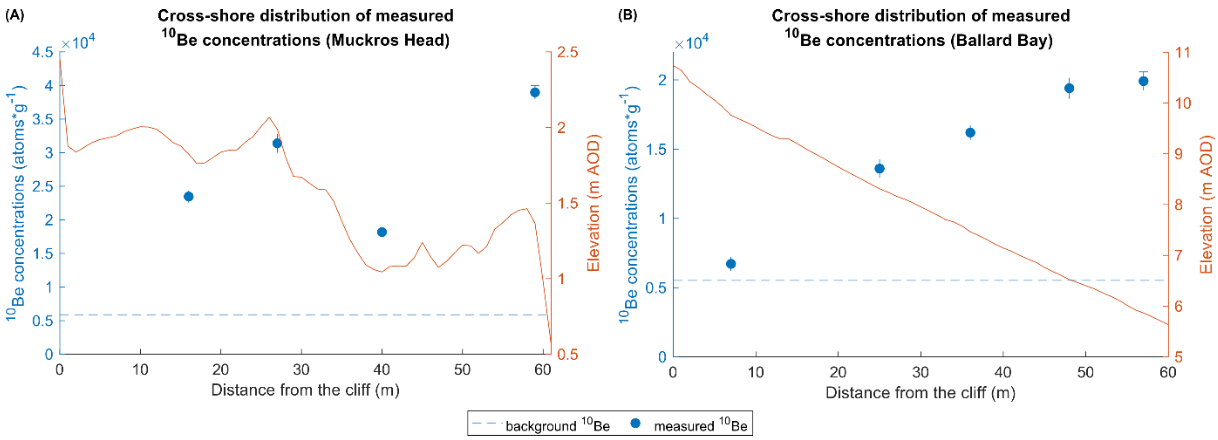

Figure 4: Cross-shore distributions of measured, uncorrected ^{10}Be concentrations (± 1σ) at (A) Muckros Head and (B) Ballard Bay. Elevations are measured as m AOD Malin Head.

Table 3 (next page): ^{10}Be sample details and nuclide data for the Muckros Head and Ballard Bay samples. MUC-5 and BAL-6 (bold) are shielded samples for quantifying background ^{10}Be concentrations. BAL-05 (italics) was excluded from further analysis due to unsuccessful measurement; BAL-7 was sampled and measured as replacement.

https://doi.org/10.5194/egusphere-2026-3761
Preprint. Discussion started: 15 September 2026

Sample ID (Blank)	LAT	LON	Elevation (m AOD Malin Head)	Sample thickness (cm)	Density (g cm^{-2})	Quartz weight (g)	^{9}Be added (µg)	$^{10}Be/^{9}Be \pm 1\sigma$ (10^{-14})	Blank corrected [^{10}Be] ±1σ (10^4) (atoms g^{-1} quartz)	Background and thickness corrected [^{10}Be] ±1σ (10^4) (atoms g^{-1} quartz)
MUC-1 (B5)	54.61008	-8.59245	1.31	3.2	2.7	30.41199	0.24354	7.36 ± 0.19	3.90 ± 0.10	3.23 ± 0.13
MUC-2 (B5)	54.60993	-8.59229	1.06	3.0	2.7	29.68183	0.24490	3.40 ± 0.12	1.82 ± 0.07	1.20 ± 0.10
MUC-3 (B5)	54.60983	-8.59219	1.93	2.8	2.7	30.02369	0.24902	5.75 ± 0.25	3.14 ± 0.14	2.50 ± 0.16
MUC-4 (B5)	54.60974	-8.59211	1.63	3.5	2.7	29.80732	0.39055	2.74 ± 0.10	2.35 ± 0.89	1.71 ± 0.12
MUC-5 (B9)	**54.60963**	**-8.59203**	**1.67**	**3.3**	**2.7**	**28.56771**	**0.24949**	**1.10 ± 0.10**	**0.59 ± 0.08**	
BAL-1 (B195B)	52.74094	-9.60613	5.13	2.5	2.7	23.3733	0.13214	5.68 ± 0.19	1.99 ± 0.07	1.37 ± 0.08
BAL-2 (B195B)	52.74093	-9.60598	5.46	4.3	2.7	22.0949	0.13240	5.23 ± 0.20	1.94 ± 0.08	1.35 ± 0.08
BAL-3 (B195B)	52.74093	-9.60582	5.95	4.4	2.7	22.5420	0.13233	4.46 ± 0.15	1.62 ± 0.05	1.02 ± 0.07
BAL-4 (B195B)	52.74094	-9.60564	7.18	3.1	2.7	25.4712	0.13193	4.25 ± 0.20	1.36 ± 0.07	0.77 ± 0.08
BAL-5 (B195B)	*52.74098*	*-9.6055*	*8.05*	*3.3*	*2.7*	*20.2578*	*0.13203*			
BAL-6 (B195B)	**52.74099**	**-9.60535**	**9.85**	**4.8**	**2.7**	**23.3038**	**0.13291**	**1.61 ± 0.11**	**0.55 ± 0.04**	
BAL-7 (B21)	52.74111	-9.60547	8.57	4.9	2.7	20.15767	0.10508	2.29 ± 0.13	0.72 ± 0.05	0.17 ± 0.06
B5							0.24759	0.11 ± 0.02		
B9							0.24715	0.10 ± 0.02		
B21							0.10490	0.22 ± 0.03		
B195B							0.13292	0.07 ± 0.02		

https://doi.org/10.5194/egusphere-2026-3761
Preprint. Discussion started: 15 September 2026

4.3 Modelled cosmogenic ^{10}Be concentrations

For Muckros Head, the closest alignment between measured and modelled ^{10}Be concentrations corresponds to a recent retreat rate of 1 mm yr^{-1} (Table 4). Applying higher retreat rates results in growing disparity between measured and modelled values, with simulations either (a) predicting ^{10}Be concentrations that are significantly lower than the measured values or (b) failing to reproduce the full profile length.

For Ballard Bay, the strongest similarities between measured and modelled ^{10}Be concentrations result from a recent cliff retreat rate of 5 mm yr^{-1}. While application of a 1 mm yr^{-1} rate (the optimal value for Muckros Head) can yield reasonable results for Ballard Bay in certain model-scenario combinations, the best-fitting model fails to cover the profile's full length. Running a recent retreat rate of 1 mm yr^{-1}, the model output that fits the measured ^{10}Be data most closely and also spans the full profile exhibits a significantly higher MSD than does the best-fit output assuming a recent rate of 5 mm yr^{-1} (Table 3). Finally, we note that simulations incorporating higher recent cliff retreat rates (a few centimetres or more annually) predicted ^{10}Be concentrations that are consistently lower than measured values and/or do not span the full profile.

https://doi.org/10.5194/egusphere-2026-3761
Preprint. Discussion started: 15 September 2026

Table 4: Summary of best-fit results for various estimates of recent cliff retreats rates at Muckros Head and Ballard Bay. All model runs for Muckros Head including the outlier sample MUC-2. The best-fit model runs are marked bold.

Field site	Estimated recent cliff retreat rate (mm yr^{-1})	Best fitting recent cliff retreat rate (mm yr^{-1})	Shore platform scenario	Cliff retreat scenario	Initial cliff retreat rate (mm yr^{-1})	MSD (atoms g^{-1})^2	Figures
Muckros Head	**1**	**1.0 ± 0.3**	**Shore platform widening**	**Deceleration**	**14 ± 5**	**5.00*10^7**	**Figure 5, Figure 6**
	5	5 ± 2	Shore platform widening	Deceleration	10 ± 4	7.19*10^7	Figure A1, Figure A2
	10	10 ± 5	Steady-state	Acceleration	3 ± 1	1.06*10^8	Figure A3, Figure A4
	50	10 ± 6	Shore platform widening	steady cliff retreat	10 ± 6	4.02*10^8	Figure A5, Figure A6
Ballard Bay	1	12 ± 3	Steady-state	Steady cliff retreat	12 ± 3	9.19*10^6	Figure A7, Figure A8
	5	**5.0 ± 0.4**	**Steady-state**	**Deceleration**	**25 ± 2**	**1.22*10^6**	**Figure 5, Figure 6**
	10	10 ± 2	Zero platform erosion	Deceleration	40 ± 8	6.79*10^6	Figure A9, Figure A10
	50	20 ± 6	Steady-state	steady cliff retreat	20 ± 6	1.45*10^7	Figure A11, Figure A12

When applying a recent retreat rate of 1 mm yr^{-1} to Muckros Head, all three platform evolution models (no platform erosion, steady-state and shore platform widening) exhibit a profound increase in ^{10}Be concentration under those scenarios in which cliff retreat accelerates. In such cases, the modelled concentrations are routinely higher than measured values and often cannot be computed for the entire length of the transect, especially when using the 'zero platform erosion' model. Steady-retreat scenarios tend to underestimate ^{10}Be concentrations in all three models, showing lower concentrations than measured; these scenarios generally resulting in high similarity between measured and modelled ^{10}Be concentration in conjunction with strongly decelerating retreat. Meanwhile,

https://doi.org/10.5194/egusphere-2026-3761
Preprint. Discussion started: 15 September 2026

the 'platform widening' model tends to overestimate ^{10}Be concentrations under scenarios of decelerating retreat and fails to reconstruct the full profile (Figure 5).

Applying a recent cliff retreat rate of 5 mm yr^{-1} to Ballard Bay, the 'zero platform down-wearing' model and steady retreat scenarios tend to underestimate ^{10}Be concentrations in all model runs. The 'steady-state' model predicts a good fit when combined with cliff retreat deceleration, but underestimates nuclide concentrations under steady retreat conditions, and overestimates concentrations under steadily high and accelerating retreat scenarios. Like the 'steady-state' model, the 'platform widening' model also underestimates ^{10}Be concentrations under scenarios of steady and decelerating retreat, while overestimating values under steadily high and accelerating retreat scenarios. All model-scenario combinations exhibit a clear rise in ^{10}Be concentration towards the outer platform (Figure 5).

https://doi.org/10.5194/egusphere-2026-3761
Preprint. Discussion started: 15 September 2026

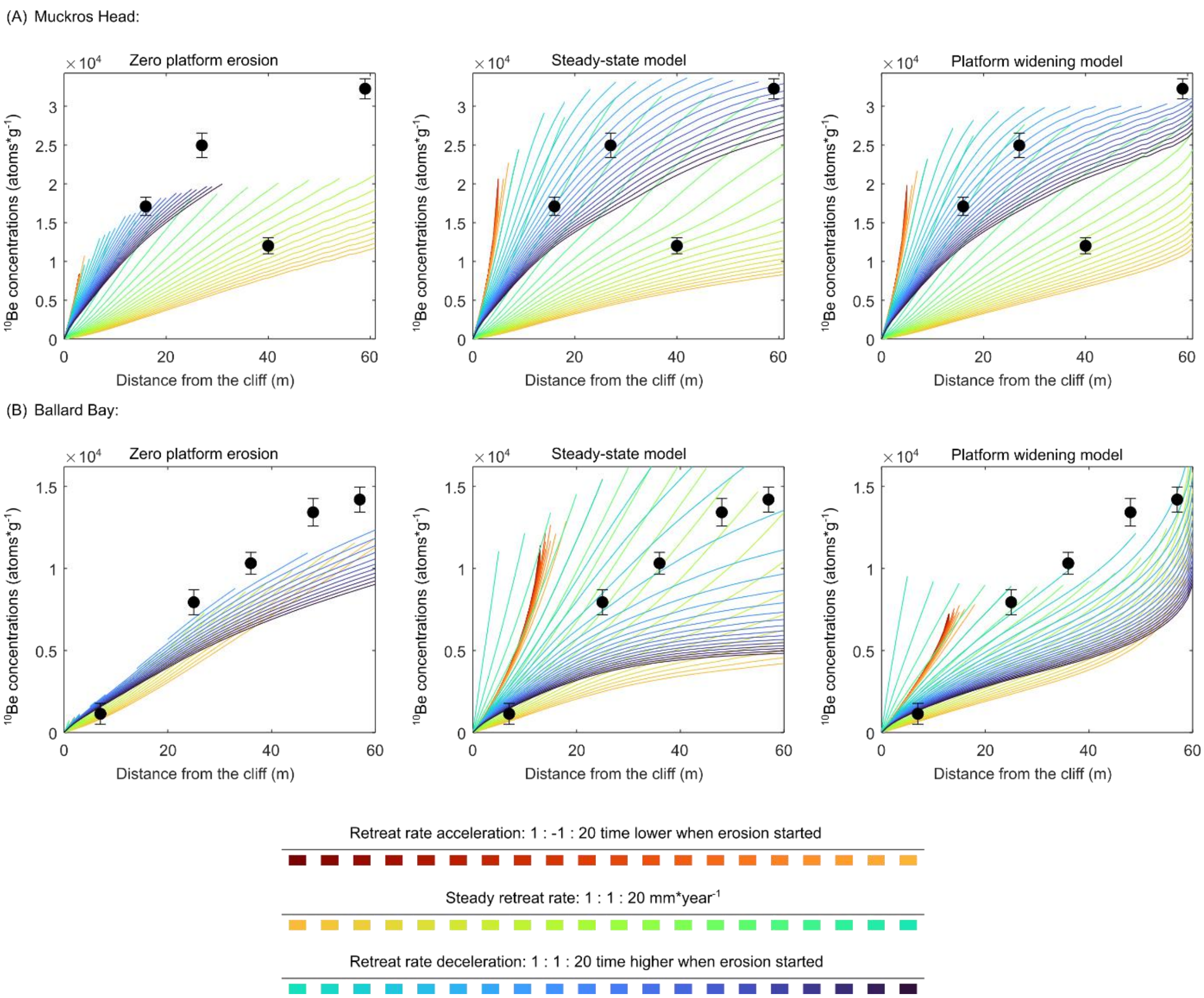

Figure 5: Modelled and measured ^{10}Be concentrations. (A) At Muckros Head, the best fitting results are calculated when applying a recent retreat rate of 1 mm yr^{-1} for deceleration and acceleration scenarios. (B) At Ballard Bay, the best fitting results are calculated when applying a recent retreat rate of 5 mm yr^{-1} for deceleration and acceleration scenarios.

4.4 Long term cliff retreat rates and shore platform evolution

For both Muckros Head and Ballard Bay, comparison of modelled and measured ^{10}Be concentrations reveals that the greatest degree of similarity (low MSD values) is achieved under decelerating cliff retreat scenarios, whereas steady-state simulations typically produce higher MSD values. At both sites, simulations incorporating

https://doi.org/10.5194/egusphere-2026-3761
Preprint. Discussion started: 15 September 2026

accelerating retreat failed to predict ^{10}Be concentrations for the entirety of the shore platform transects, thereby precluding calculation of MSD.

At Muckros Head, the best fit between measured and simulated ^{10}Be concentrations (MSD = $5*10^7$ (atoms $g^{-1})^2$, NRMSD = 0.3495) corresponds to decelerating cliff retreat over the course of the Holocene coupled with widening of the shore platform (Figure 6). According to this optimal configuration, cliff retreat decelerated from an initial rate of 14 ± mm yr^{-1} to a late Holocene rate of 1.0 ± 0.3 mm yr^{-1}.

Holocene deceleration of cliff retreat is also implicated for Ballard Bay, where the optimal fit (MSD = $1.22*10^6$ (atoms $g^{-1})^2$, NRMSD = 0.0847) corresponds to decreasing cliff retreat alongside steady-state down-wearing of the shore platform. According to this simulation, the cliff retreat decelerated from an initial rate of 25 ± 2 mm yr^{-1} in the early Holocene to a more recent rate of 5.0 ± 0.4 mm yr^{-1} (Figure 6).

https://doi.org/10.5194/egusphere-2026-3761
Preprint. Discussion started: 15 September 2026

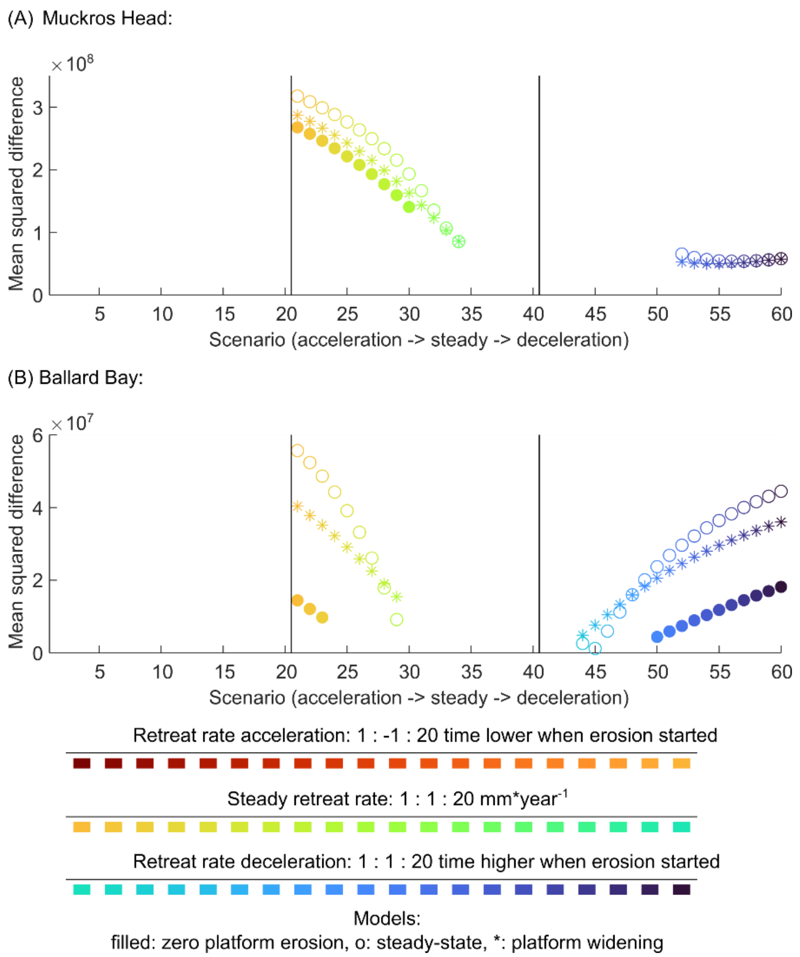

Figure 6: Mean squared differences between measured and modelled 10Be concentrations for (A) Muckros Head and (B) Ballard Bay. (A) The best-fit scenarios for Muckros Head describe decelerating cliff retreat during the Holocene, from an initial rate 14 ± 5 mm yr^{-1} to a recent rate of 1.0 ± 0.3 mm yr^{-1}, coincident with shore platform widening (MSD = 5*10^{7} (atoms g^{-1})^{2}). (B) For Ballard Bay, the best fit-scenarios describe decelerating cliff retreat during the Holocene, from initially 25 ± 2 mm yr^{-1} to a recent rate of 5.0 ± 0.4 mm yr^{-1}, coincident with shore platform widening (MSD = 1.22*10^{6} (atoms g^{-1})^{2}).

4.5 Wave conditions

According to wave buoy data from the three stations offshore of Mayo and Clare (Figure 1), mean wave direction at both field sites is W–WNW and daily mean Hs is 2–4 m. The highest daily mean Hs (10.5 ± 1.5 m) was recorded by the AMETS Berth A wave buoy, which also recorded the greatest deviation in wave direction from the W–WNW average (Figure 7).

https://doi.org/10.5194/egusphere-2026-3761
Preprint. Discussion started: 15 September 2026

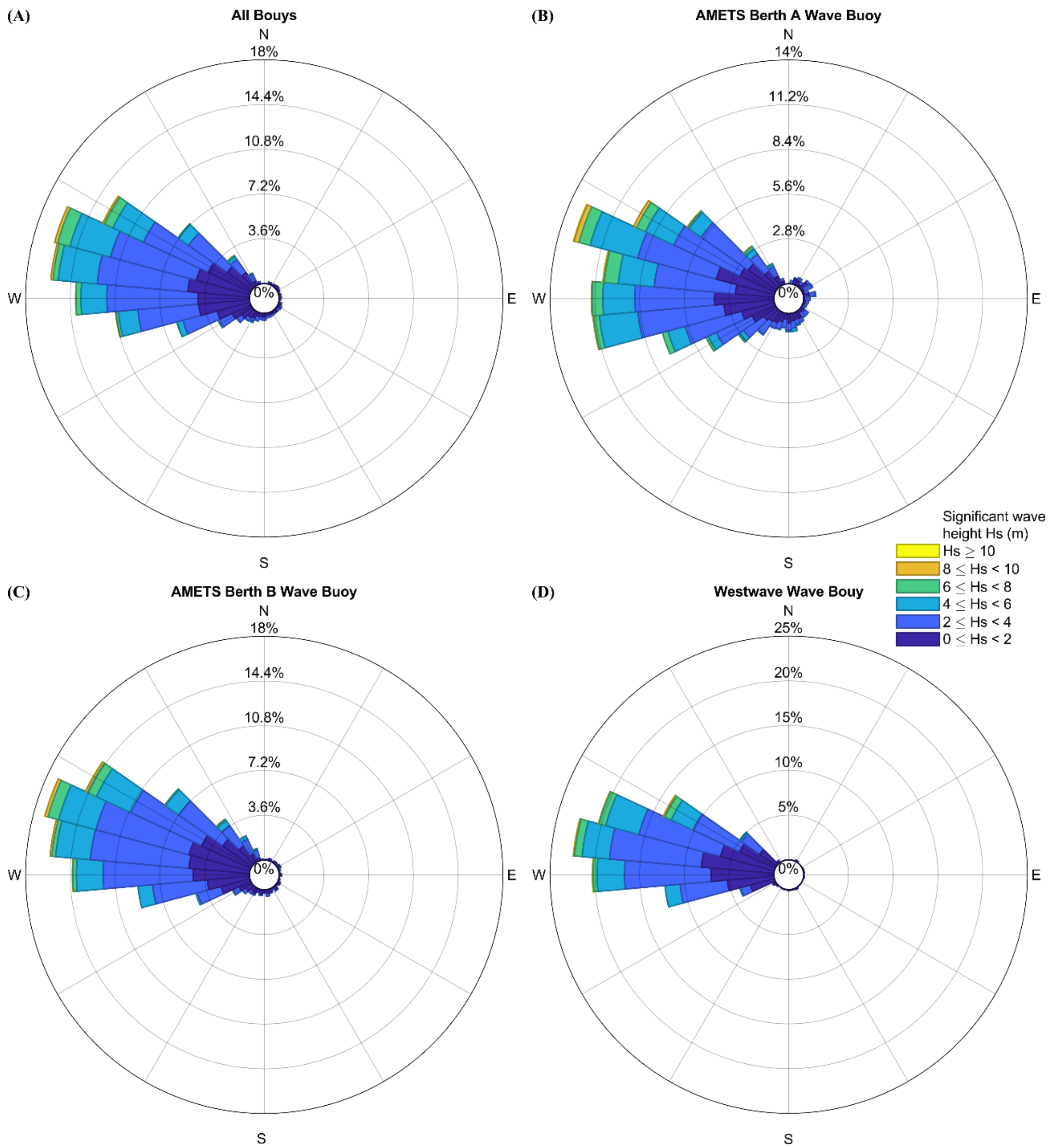

Figure 7: Significant wave height, *H_s*, and mean wave direction data derived from quasi-daily observations by the three wave buoys indicated in Figure 1. At all three sites, wave direction is predominantly from the W–WNW, with Hs values of 2–4 m (DigitalOcean.ie, 2025). (A) Daily mean *H_s* between 14/05/2015 and 22/04/2025, summarised from the three wave buoys. (B) Daily mean *H_s* at the AMETS Berth A wave buoy, between 19/05/2019 and 22/07/2025. (C) Daily mean *H_s* at the AMETS Beth B wave buoy, from 14/05/2015 to 22/07/2025. (D) Daily mean *H_s* at the Westwave wave buoy, between 15/05/2015 and 37/03/2019. Graphs were computed with "Wind Rose" (Pereira, 2025).

https://doi.org/10.5194/egusphere-2026-3761
Preprint. Discussion started: 15 September 2026

5 Discussion

5.1 Holocene cliff retreat

Since the inheritance of cosmogenic ^{10}Be from prior periods of exposure (e.g., the last interglacial) would be manifested in a transect as a distinct step in nuclide concentrations (Regard et al., 2012; Hurst et al., 2016; Swirad et al., 2020; Shadrick et al., 2022; Jeong et al., 2026) the steady outward rise in ^{10}Be concentration exhibited by the Muckros Head and Ballard Bay transects indicates that both shore platforms are primarily Holocene structures. Both sites show a trend of declining cliff retreat rate during the Holocene: cliff retreat decreased from 14 to 1 mm yr^{-1} at Muckros Head, and from 25 to 5 mm yr^{-1} at Ballard Bay. The declaration of cliff retreat rates at both sites mirrors the slowing down of Holocene RSL rise; the slightly faster deceleration at Muckros Head reflects the RSL curves reported by Shennan et al. (2018), which exhibit continuously higher Holocene RSL at Muckros Head than at Ballard Bay (Table 1). The northern part of Ireland, including Muckros Head, experienced a later onset of subaerial emergence than southern regions (e.g., Ballard Bay) due to greater glacio-isostatic depression during the last glacial maximum (Bradley et al., 2011). We propose that an earlier deglaciation and minimal glacio-isostatic depression set Ballard Bay above RSL and out of the reach of marine influences until RSL rise caught up. After deglaciation at Muckros Head, the higher RSL led to a stronger marine impact and an earlier start of marine driven erosion, despite a faster postglacial rise in southern County Clare than in western Donegal. Ultimately, when RSL rise induced cliff retreat at Ballard Bay in mid-Holocene, the faster RSL rising rates resulted in higher contemporary cliff retreat rates, compared to Muckros Head. Similar relationships between cliff retreat rates and RSL have been reported repeatedly, but they appear to be highly site specific and not always significant (Swirad et al., 2020; Shadrick et al., 2021; Jeong et al., 2024). For example, Swirad et al. (2020) reported a steady retreat rate during the Holocene from a sandstone cliff at Hartle Loup, England despite decreasing rate of RSL rise. In contrast, using the same methodology and model, Jeong et al. (2024) reported a clear relationship between RSL and ^{10}Be concentrations on a shore platform at Yeongdeok-gun, South Korea, where rising RSL during the Holocene coincided with accelerating cliff retreat. Similarly, using a process-oriented model approach Shadrick et al. (2021), concluded that declining Holocene retreat rates of sandstone cliffs at Scalby and Bedford, England, reflect decelerating RSL rise.

Finally, the anomalously low ^{10}Be concentration of sample MUC-2 is most likely the product of block removal subsequent to the platform's formation, the saw-toothed shape of the resulting ^{10}Be concentration curve being characteristic of this erosion process (Swirad et al., 2020). Calculating sample MUC-2 as a simple surface-exposure age, using version 3 of the University of Washington online calculator (https://hess.ess.washington.edu/,

https://doi.org/10.5194/egusphere-2026-3761
Preprint. Discussion started: 15 September 2026

last access 05/02/2026) (Balco et al., 2008) and Rannoch Moor production rate (Putnam et al., 2019), indicates that block detachment occurred during the middle Holocene (3.1 ± 0.4 ka with St scaling).

5.2 Marine drivers on erosion

Under modern conditions, the shore platforms extend up approximately 3.5 m at Muckros Head and 10.5 m at Ballard Bay to above sea level at their innermost points. Nevertheless, geomorphic evidence from both sites indicates sporadic marine incursions and marine-driven erosion due to large swash zones (especially Ballard Bay), particularly during spring tides and storm surges. Block removal from layered shore platforms, such as at Muckros Head, is most likely the product of waves action (Knight and Burningham, 2011; Buchanan et al., 2020) and results in the generation of loose boulders, which are subsequently transported waves and ultimately form coastal boulder deposits (CBD). Since the size of CBDs depends on the significant wave height, they are used as an indicator for storm surges and storms wave (Paris et al., 2011; Cox et al., 2018; Kennedy et al., 2021; Van Blunk et al., 2021). At Muckros Head, we interpreted a boulder on the inner shore platform as a cliff-detachment block type CBD (Cox et al., 2018), based on its composition reflecting the local cliff material, its mass, and its position (Figure 8). This CBD is currently situated approximately 4 m in front of the cliff base, has a volume of approximately 38 m^3 (based on ABC-dimensions) and weighs ~100 tons, based on the density of quartz (2.65 g cm^{-3}). A CBD of these dimensions on the upper shore platform indicates that the entire platform is susceptible to storm waves that drive coastal erosion and cliff retreat.

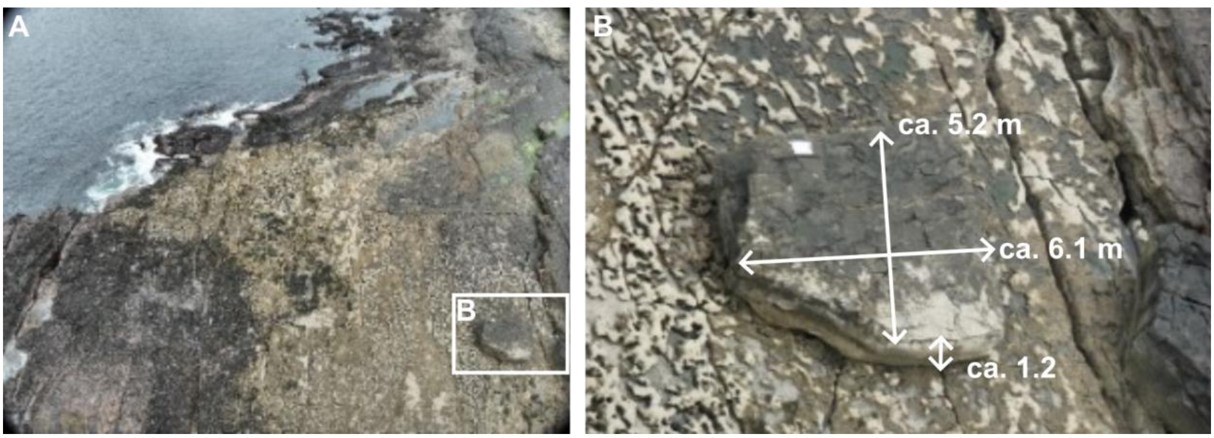

Figure 8: (A) A potential coastal boulder deposit (CBD) on the upper shore platform at Muckros Head, close to the cliff base. The CBD indicates that storm waves with high significant wave heights impact the full width of the shore platform. (B) Based on its ABC-dimensions, the boulder has a volume of approximately 38 m^3, corresponding to a mass of approximately 100 tons.

https://doi.org/10.5194/egusphere-2026-3761
Preprint. Discussion started: 15 September 2026

At Ballard Bay, the comparatively smooth shore platform allows a wide swash zone, and broken waves can reach the cliff base regularly. The absence of talus slopes at the cliff base and smaller clasts on the upper shore platform is further indication that waves regularly reach relatively high elevations; such wave action mobilises sediment and ultimately drives clast abrasion of the platform surface. This process is confirmed by clast abrasion experiments at Ballard Bay, which quantify wave-driven erosion on the upper part of the shore platform, particularly during storms (Cullen and Bourke, 2018). Furthermore, observed clast abrasion at Ballard Bay supports the cliff retreat rate in the best fitting modelled results, suggesting that the long-term reduction in cliff retreat rate has been accompanied by platform down-wearing. Due to high waves and wave run-up at the time of sampling, we could not sample the outermost Ballard Bay shore platform and so focused on the interior portion. In so doing, we acknowledge that our modelled results reflect cliff retreat independent of processes operating on the outer shore platform and thus do not span the full record of cliff evolution at this site.

Our results show that marine-driven erosion at Ballard Bay results in higher cliff retreat rates than at Muckros Head. Considering the higher elevation of the cliff base at the former and the carbonate-rich, karstified lithology at Muckros Head, one might expect the opposite pattern. Yet, Ballard Bay opens towards the west and thus receives the unfettered force of North Atlantic waves, which enter the bay with minimal deceleration and/or bending. In contrast, the Muckros Head peninsula generally, and its NW–SE-oriented shore platform specifically, experience a degree of protection from the north coast of Donegal Bay, which partially blocks waves approaching the site from WNW–NW directions. Therefore, we propose that there contrasting geographic configurations relative to the North Atlantic plausibly explain the lower long-term retreat rates at Muckros Head relative to Ballard Bay, despite the greater susceptibility of the carbonate sandstone bedrock at the former to chemical weathering.

The high cliff base elevations at both sites raise the question of the extent to which recent cliff retreat is driven by marine versus terrestrial processes. Ground water discharge, for example, is conspicuous along the cliff face at Ballard Bay and intrinsically linked to local weather conditions. Groundwater is also a credible driver of rockfall, and thus of terrestrially driven cliff retreat (Strunden et al., 2015; Young et al., 2021). Continuous analysis of the cliff face via, for example, terrestrial lidar, coupled with the magnitude/frequency/location logging of rockfalls, would help identify potential core areas of cliff erosion and potential links with such parameters as ground water discharge points, fractures, and bedding (Strunden et al., 2015; Williams et al., 2019; Mohadjer et al., 2020).

https://doi.org/10.5194/egusphere-2026-3761
Preprint. Discussion started: 15 September 2026

5.3 Model performance

In the case of Muckros Head, block detachment causes a considerable offset between simulated and measured ^{10}Be concentrations; the result is a high square difference for the MUC-2 data point under the optimal declaration scenario and a higher MSD for the model as a whole. Furthermore, while steady-state scenarios perform better for sample MUC-2, they produce a considerably worse fit for the other sample points (Figure 9).

For the majority of model-scenario combinations, square differences for Ballard Bay generally increase towards the outer platform, culminating at BAL-2 (Figure 9). This peak, which most runs failed to simulate, probably results from tide-induced variability in *in situ* ^{10}Be production (Hurst et al., 2017).

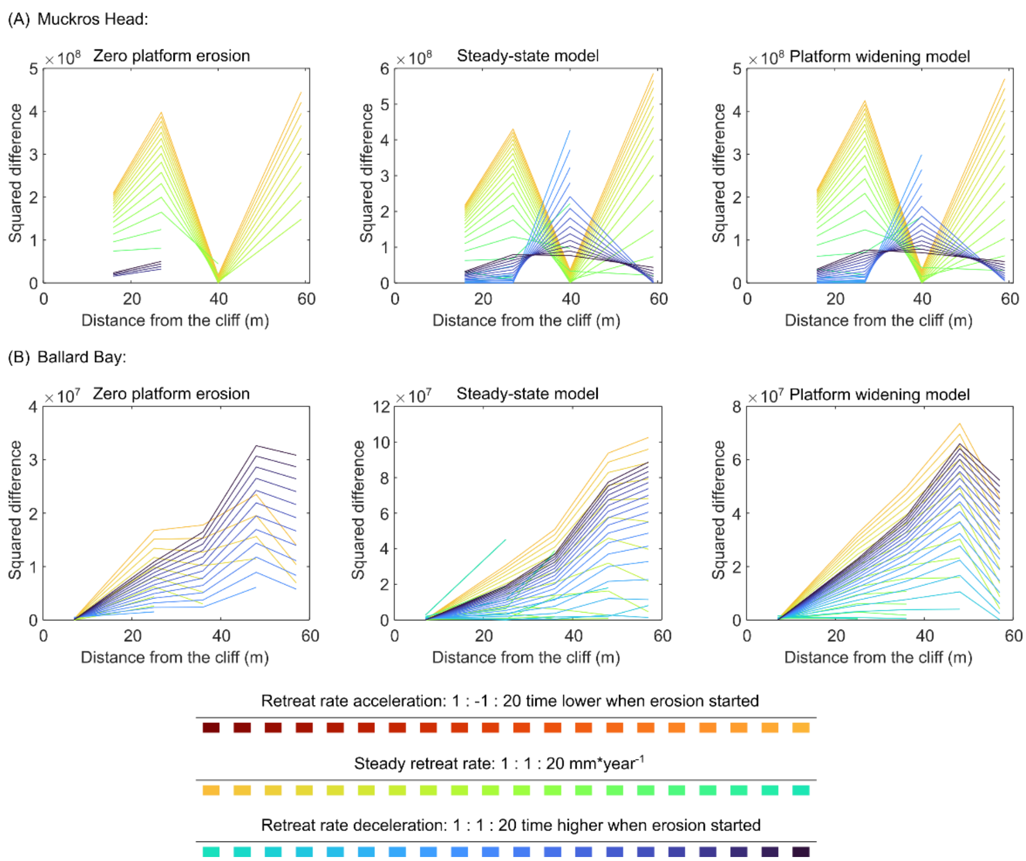

Figure 9: Squared differences across the shore platform for (A) Muckros Head and (B) Ballard Bay. (A) At Muckros Head, all scenarios show a divergence from the normal trends at the location MUC-2. While the normally good fitting decelerating cliff retreat scenarios show a high square difference for MUC-2, the less good fitting steady-state scenarios result in a lower than usual square difference. (B) At Ballard Bay, most models and scenarios show the highest squarest differences at the location BAL-2.

https://doi.org/10.5194/egusphere-2026-3761
Preprint. Discussion started: 15 September 2026

The model assumes steady retreat rates or, in cases of decelerating and accelerating retreat rates, linear changes. It neglects changing of cliff retreat rates erosion behaviour of the shore platform over time. This results in a wide range of possible platform evolution and cliff retreat scenarios with relative similar MSD. Therefore, the results represent most likely average cliff retreat rates during the Holocene (Swirad et al., 2020; Shadrick et al., 2022, 2023).

6 Conclusion

We applied a coupled cosmogenic ^{10}Be–modelling approach to reconstruct erosion histories for two hard-rock coastal sites on Ireland's western seaboard - Muckros Head and Ballard Bay. Both sites exhibit declining cliff retreat rates during the Holocene, corresponding to the regional deceleration in postglacial RSL rise. The decrease in cliff retreat is more pronounced at Muckros Head (14 → 1 mm yr^{-1}) than Ballard Bay (25 → 5 mm yr^{-1}), where Holocene RSL was lower. The modelling suggests that shore platforms developed via widening at Muckros Head, and parallel to the cliff retreat (steady-state) at Ballard Bay. Despite the location of cliff/shore platform junction at both sites extending several metres above modern sea level, the backing cliffs at each site are still impacted by marine driven erosion, the severity of which is influenced in by the shore platform morphology, lithology and exposed vs protected location. Smooth shore platforms, such as Ballard Bay, allow a wide swash zone that permits waves to reach the cliff base (even several metres above sea level) regularly, thereby inducing surface clast abrasion and cliff-base erosion. In contrast, stepped platforms like Muckros Head are more prone to block detachment, the cliff base being affected primarily by storm waves, especially when featuring a high step at the seaward edge of the shore platform.

In the context of Ireland's diverse coastal environments, we recognise that this study focuses on a relatively narrow sector, in which cliffs of similar lithology (sandstone, siltstone) are exposed to the North Atlantic Ocean. Since cliff retreat rates at both sites appear to depend largely on sea level variability and storms, studies in other settings, particularly those underlain by different lithologies and experiencing different environmental and marine conditions, are necessary to advance our understanding of hard-rock cliff erosion in Ireland.

https://doi.org/10.5194/egusphere-2026-3761
Preprint. Discussion started: 15 September 2026

Appendix

A1 Results for other recent cliff retreat rates

Muckros Head

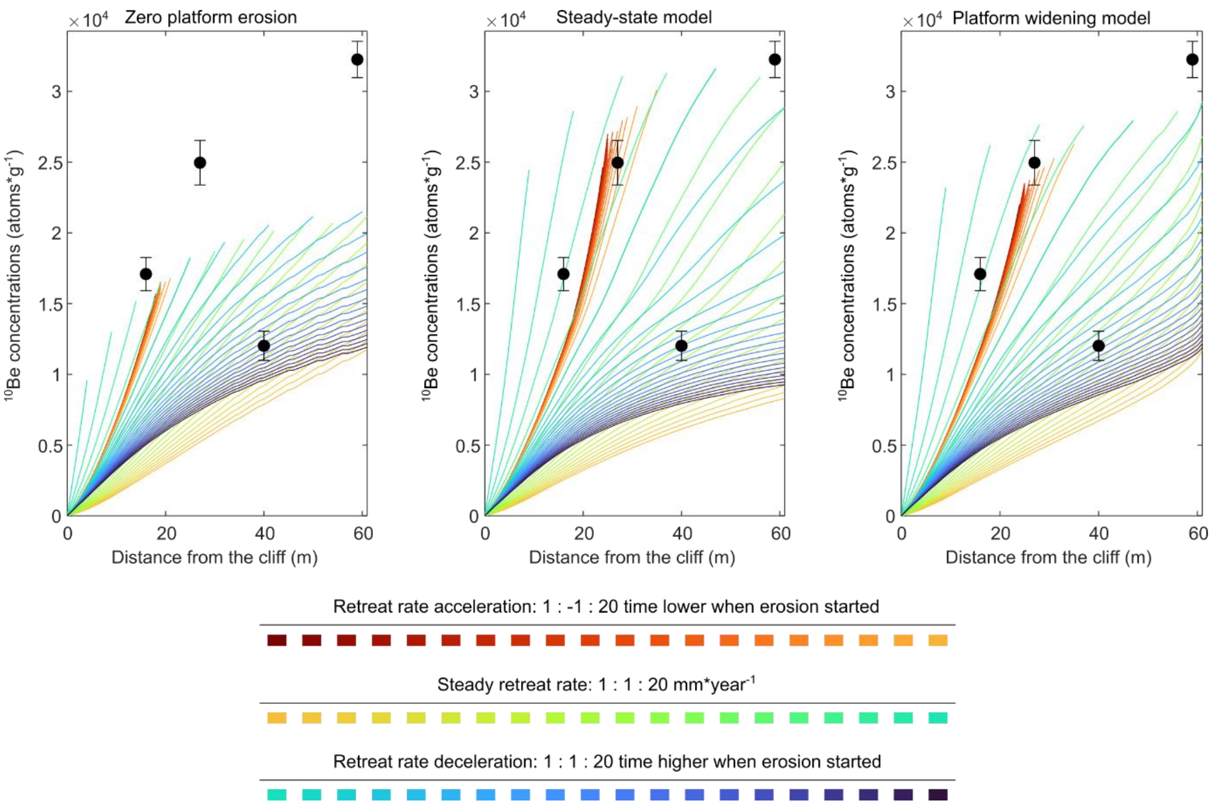

520 **Figure A1: Modelled and measured ^{10}Be concentrations for Muckros Head. Modelled for an estimated recent cliff retreat rate of 5 mm yr^{-1}.**

https://doi.org/10.5194/egusphere-2026-3761
Preprint. Discussion started: 15 September 2026

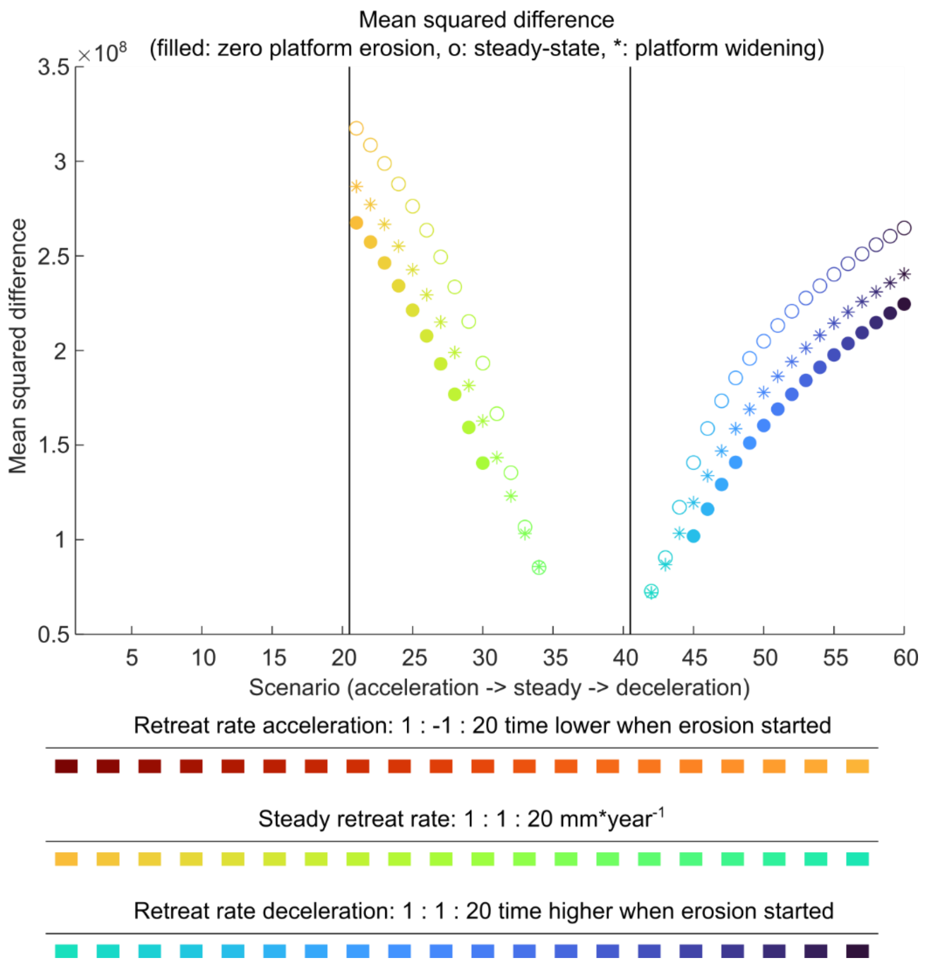

Figure A2: Mean squared differences between measured and modelled ^{10}Be concentrations for Muckros Head calculated for an estimated recent cliff retreat rate of 5 mm yr^{-1}.

525

https://doi.org/10.5194/egusphere-2026-3761
Preprint. Discussion started: 15 September 2026

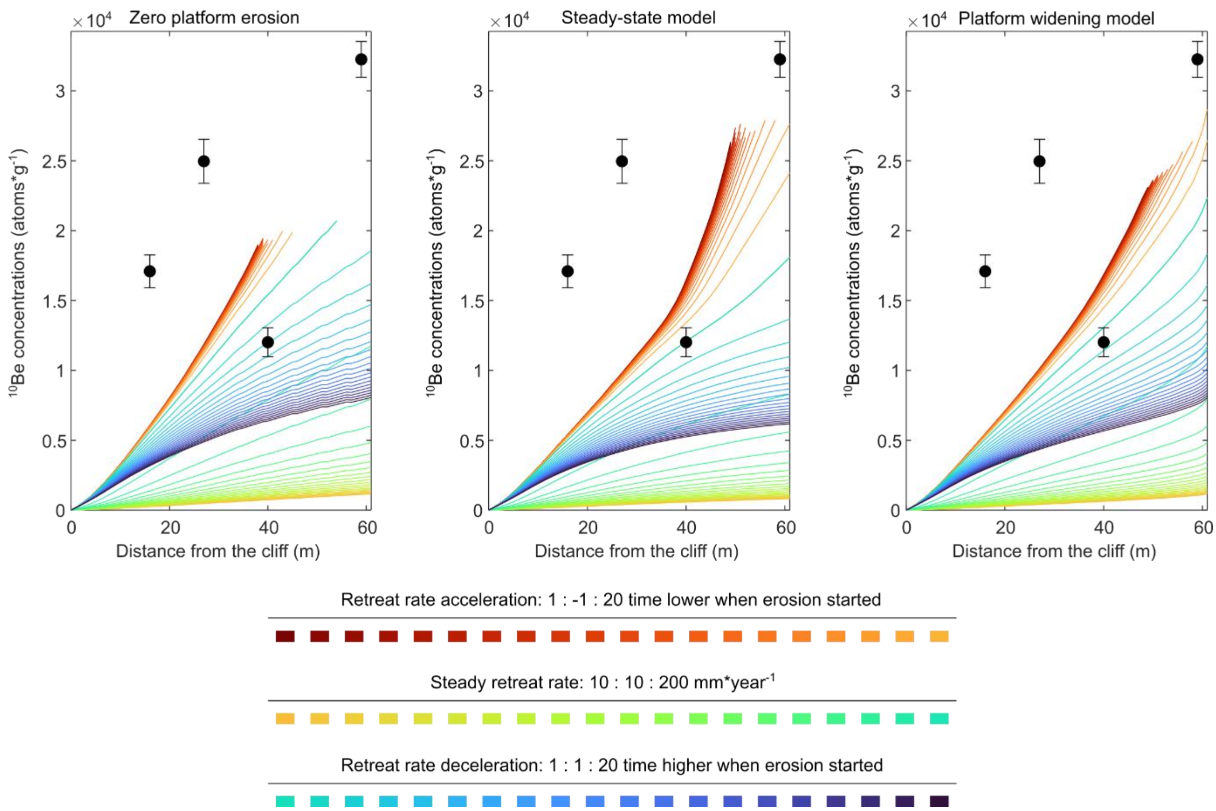

Figure A3: Modelled and measured ^{10}Be concentrations for Muckros Head. Modelled for an estimated recent cliff retreat rate for an estimated recent cliff retreat rate of 10 mm yr^{-1}.

https://doi.org/10.5194/egusphere-2026-3761
Preprint. Discussion started: 15 September 2026

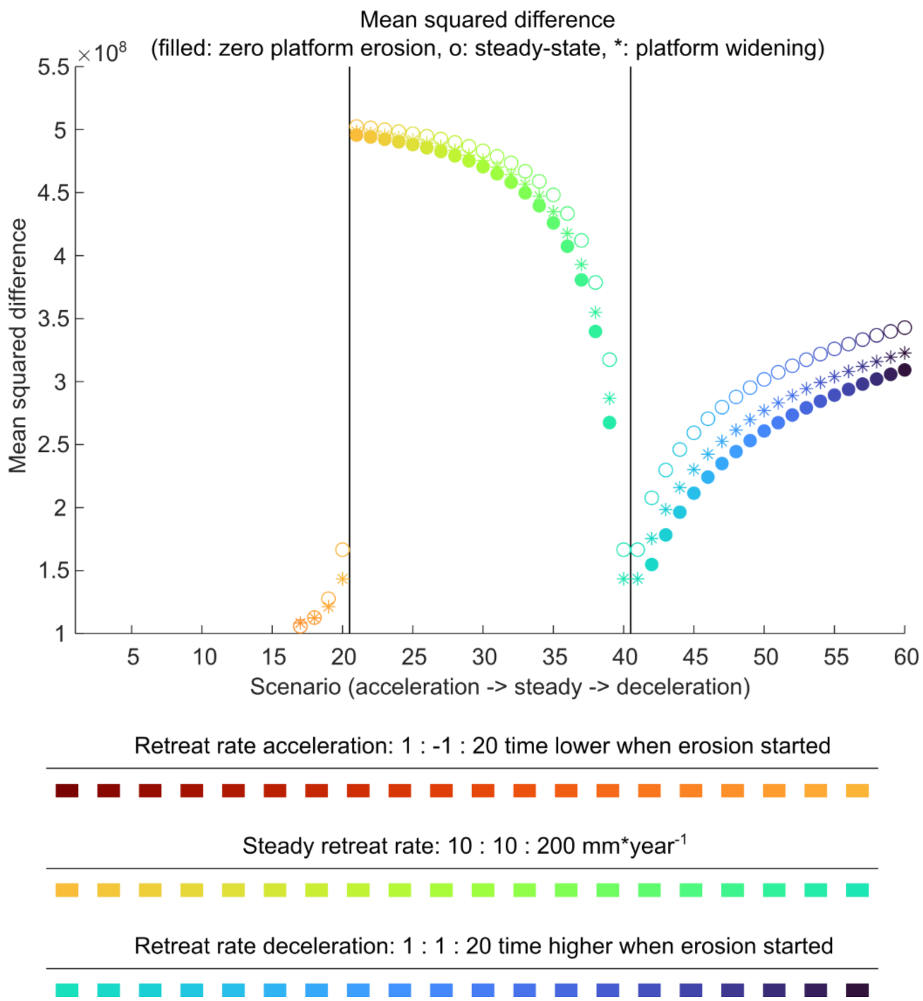

530 **Figure A4: Mean squared differences between measured and modelled ^{10}Be concentrations for Muckros Head calculated for an estimated recent cliff retreat rate of 10 mm yr^{-1}.**

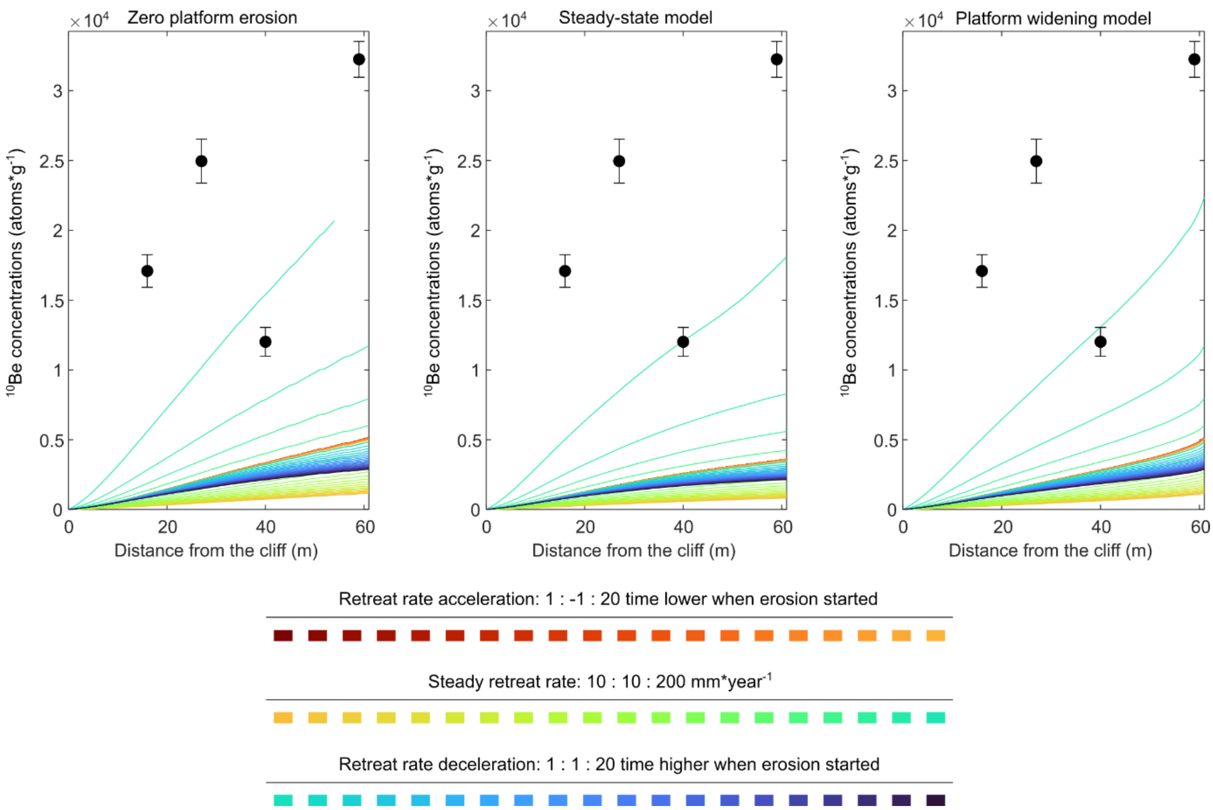

Figure A5: Modelled and measured ^{10}Be concentrations for Muckros Head. Modelled for an estimated recent cliff retreat rate of 50 mm yr^{-1}.

https://doi.org/10.5194/egusphere-2026-3761
Preprint. Discussion started: 15 September 2026

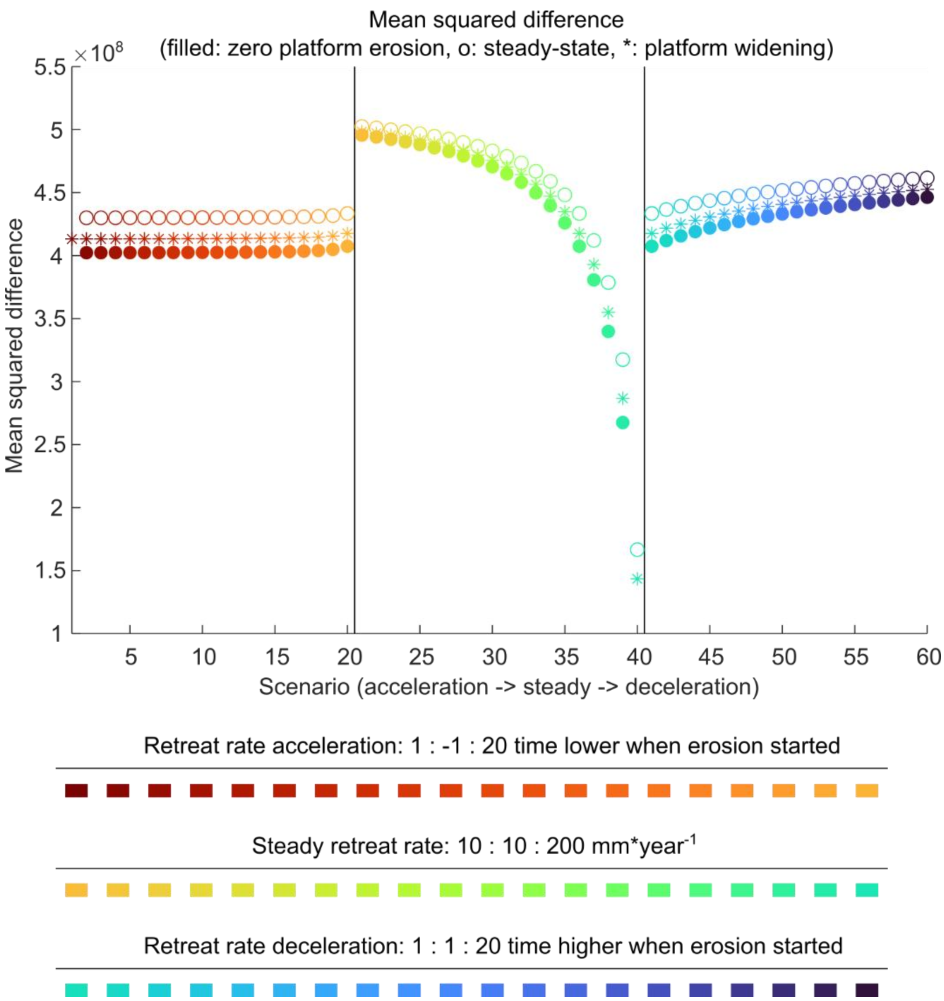

Figure A6: Mean squared differences between measured and modelled ^{10}Be concentrations for Muckros Head calculated for an estimated recent cliff retreat rate of 50 mm yr^{-1}.

540

https://doi.org/10.5194/egusphere-2026-3761
Preprint. Discussion started: 15 September 2026

Ballard Bay

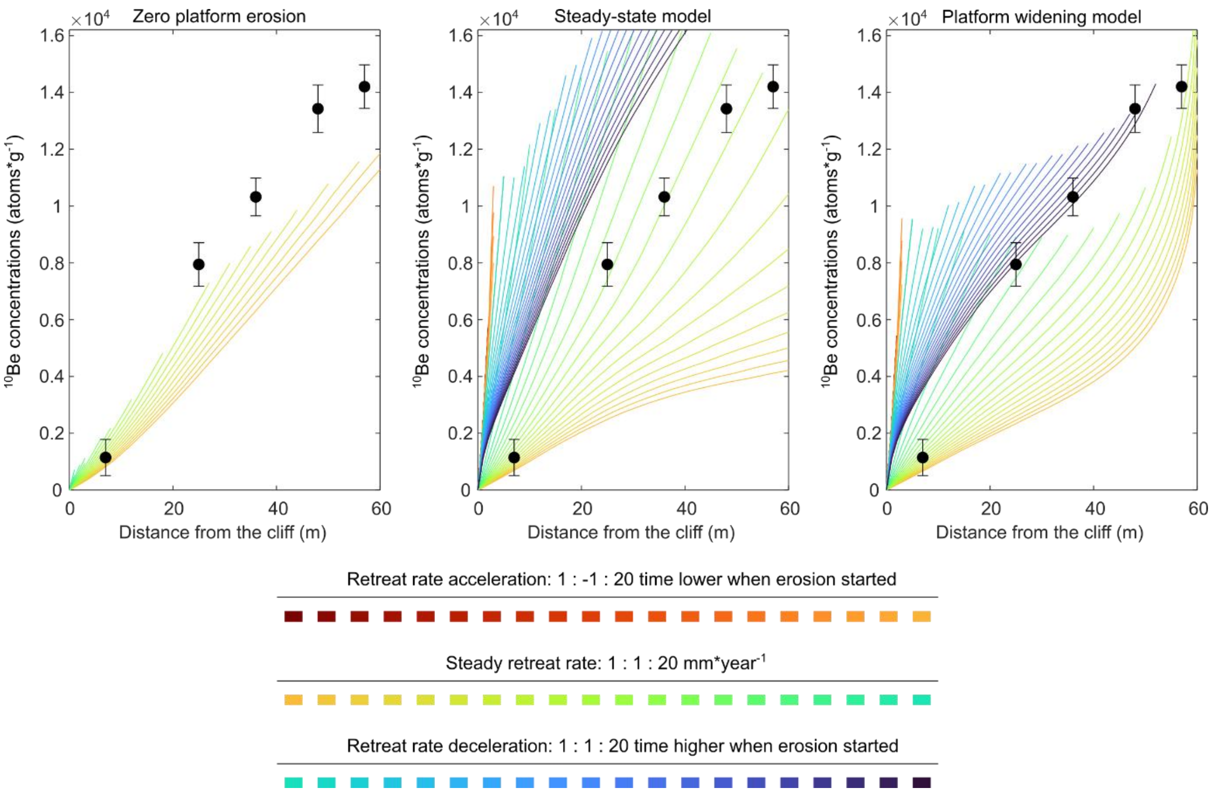

545 **Figure A7: Modelled and measured ^{10}Be concentrations for Ballard Bay. Modelled for an estimated recent cliff retreat rate. Modelled for an estimated recent cliff retreat rate 1 mm yr^{-1}.**

https://doi.org/10.5194/egusphere-2026-3761
Preprint. Discussion started: 15 September 2026

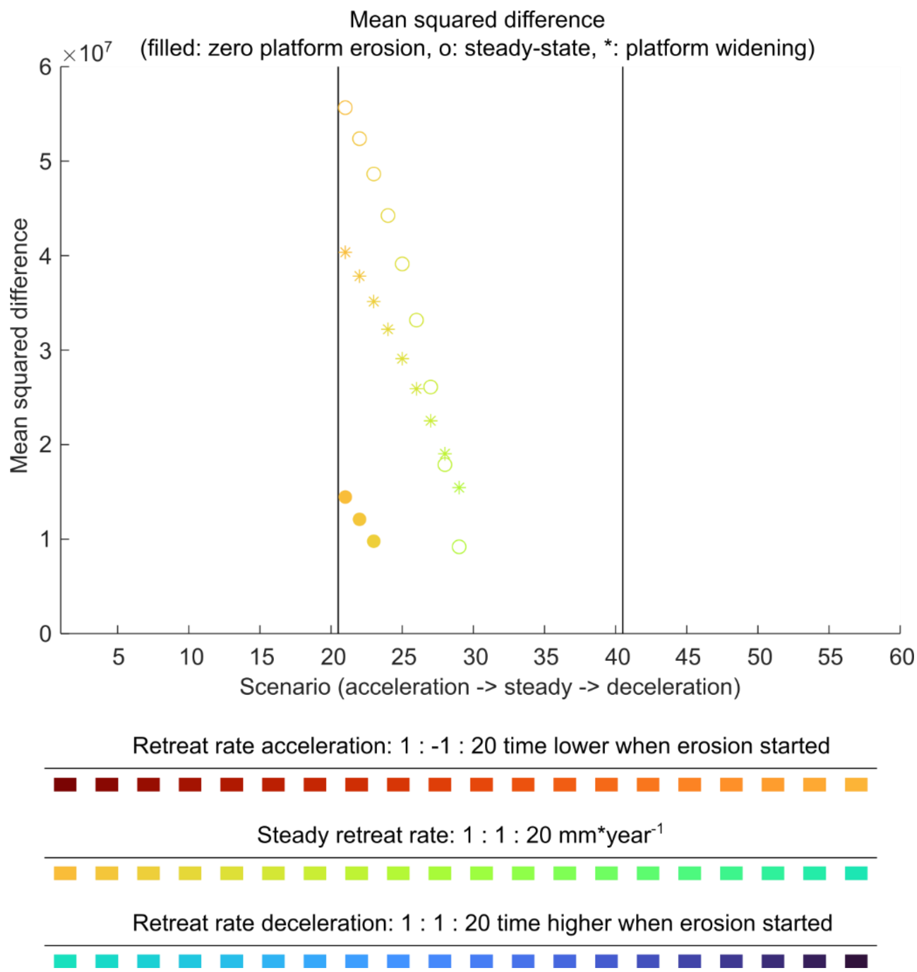

Figure A8:. Mean squared differences between measured and modelled ^{10}Be concentrations for Ballard Bay calculated for an estimated recent cliff retreat rate of 1 mm yr^{-1}.

550

https://doi.org/10.5194/egusphere-2026-3761
Preprint. Discussion started: 15 September 2026

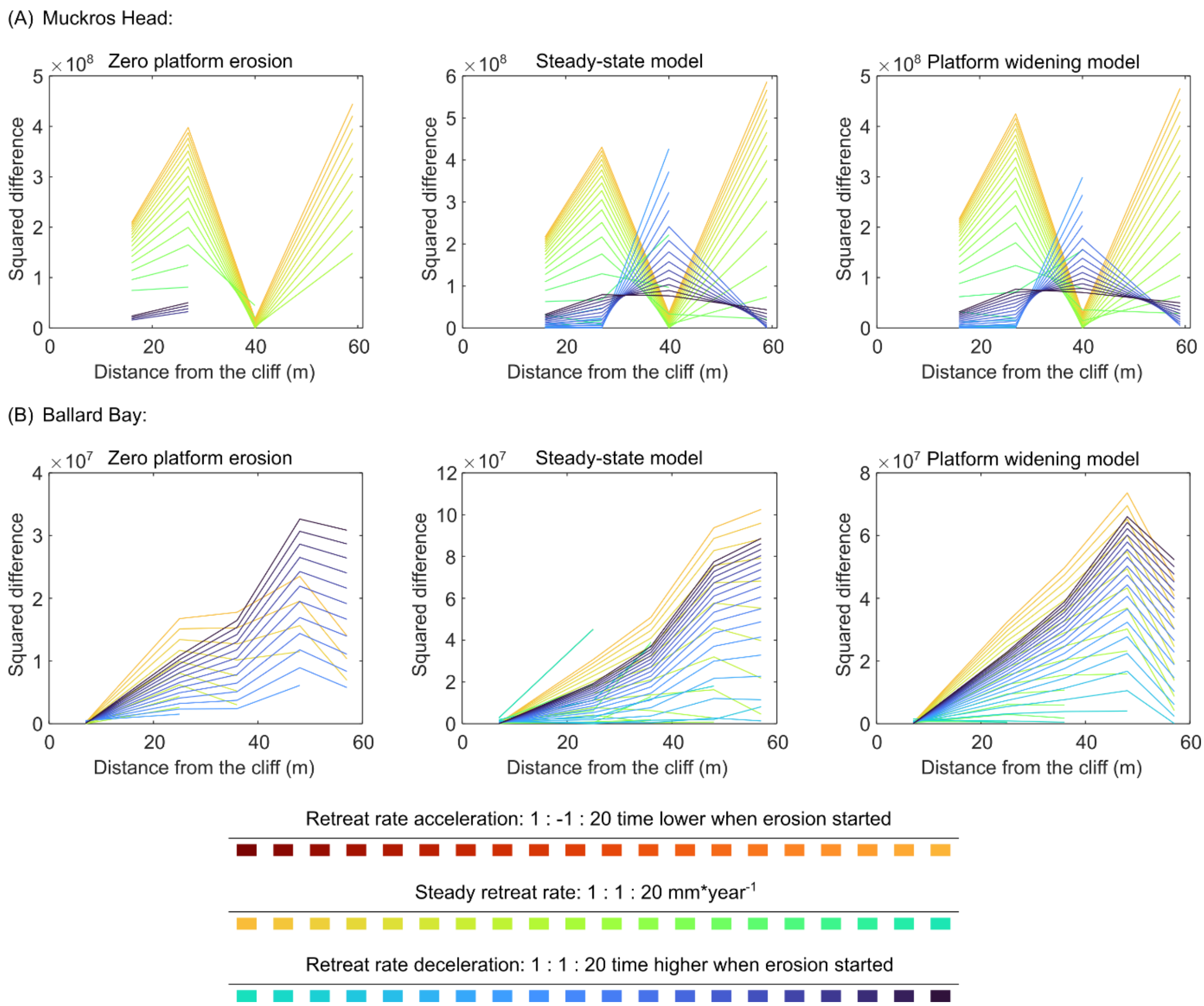

Figure A9: Modelled and measured ^{10}Be concentrations for Ballard Bay. Modelled for an estimated recent cliff retreat rate. Modelled for an estimated recent cliff retreat rate 10 mm yr^{-1}.

https://doi.org/10.5194/egusphere-2026-3761
Preprint. Discussion started: 15 September 2026

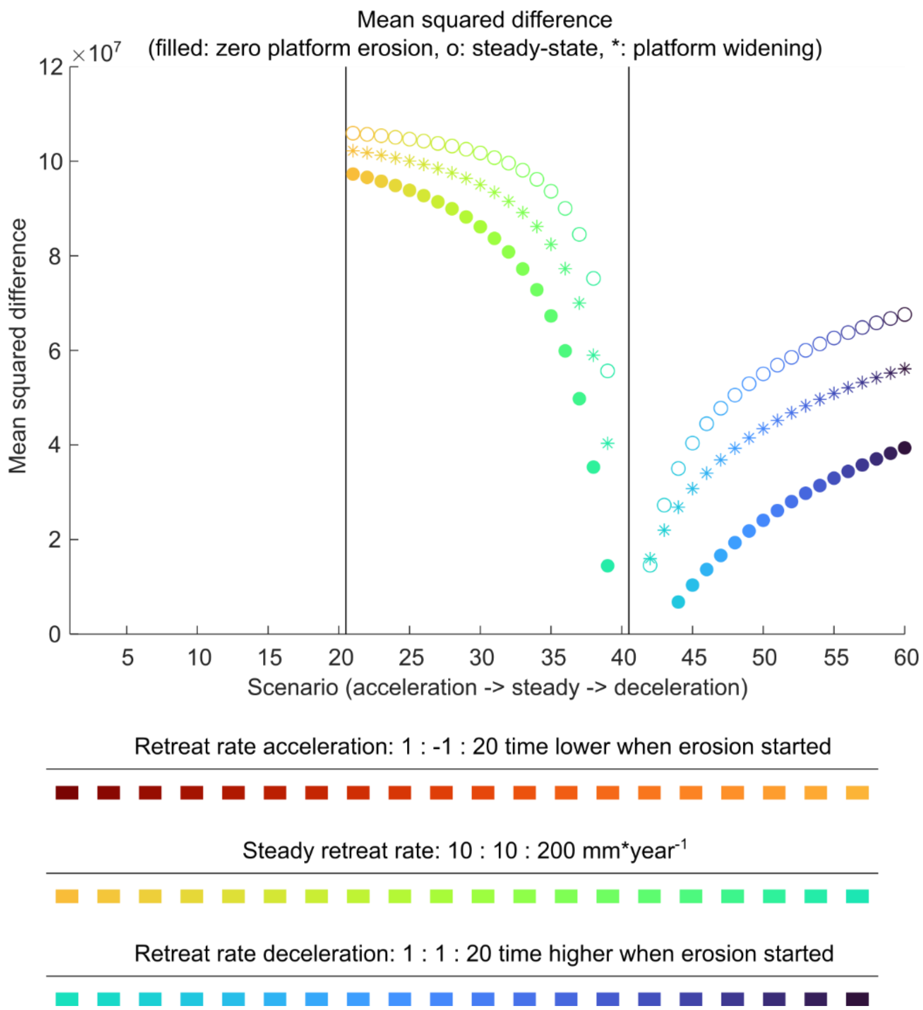

Figure A10: Mean squared differences between measured and modelled ^{10}Be concentrations for Ballard Bay calculated for an estimated recent cliff retreat rate of 10 mm yr^{-1}.

https://doi.org/10.5194/egusphere-2026-3761
Preprint. Discussion started: 15 September 2026

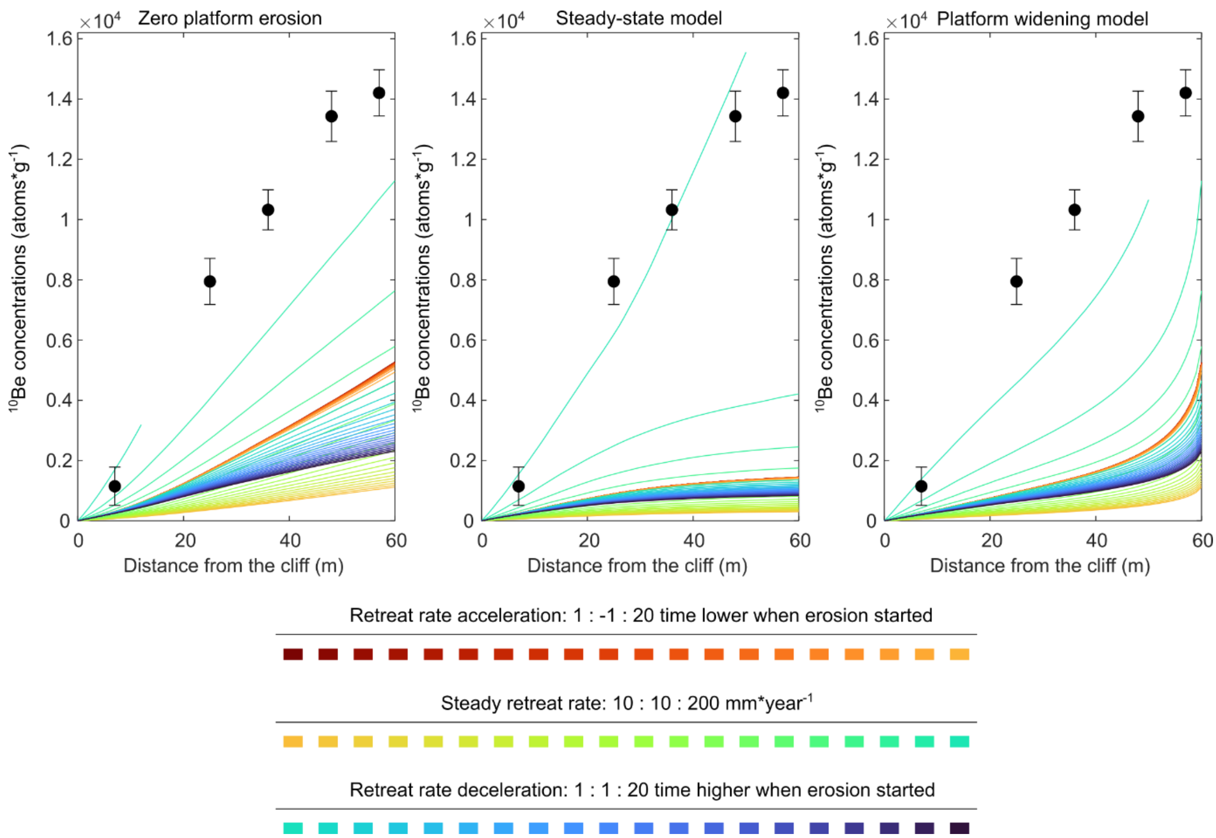

560 **Figure A11: Modelled and measured ^{10}Be concentrations for Ballard Bay. Modelled for an estimated recent cliff retreat rate. Modelled for an estimated recent cliff retreat rate 50 mm yr^{-1}.**

https://doi.org/10.5194/egusphere-2026-3761
Preprint. Discussion started: 15 September 2026

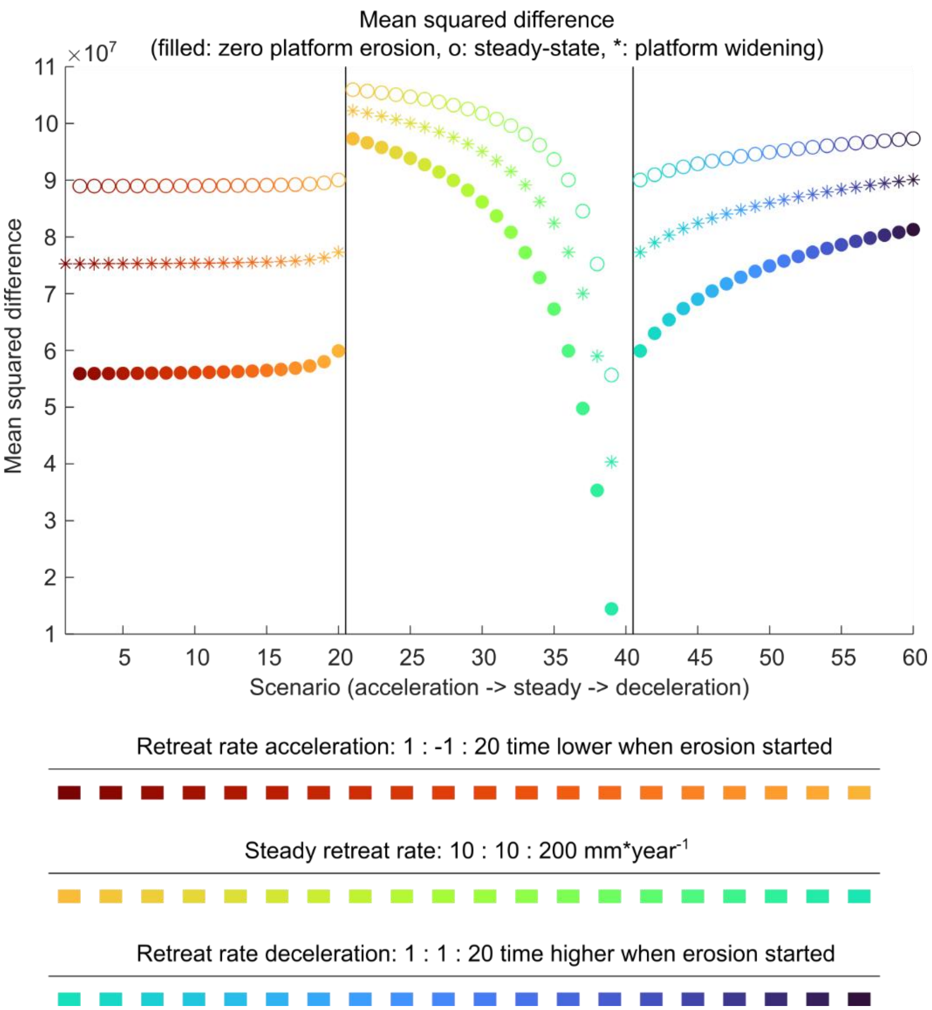

Figure A12: Mean squared differences between measured and modelled ^{10}Be concentrations for Ballard Bay calculated for an estimated recent cliff retreat rate of 50 mm yr^{-1}.

565 **Code and data availability**

All necessary DSMs, cosmogenic beryllium-10 data and codes for cliff erosion analysis can be accessed via https://doi.org/10.5281/zenodo.20844617 (Rink and Bromley, 2026).

Wave data of the respective wave buoys can be downloaded from

https://www.digitalocean.ie/Data/DownloadWaveData/AMETS%20Berth%20A%20Wave%20Buoy

570 https://www.digitalocean.ie/Data/DownloadWaveData/AMETS%20Berth%20B%20Wave%20Buoy

https://www.digitalocean.ie/Data/DownloadWaveData/Westwave%20Wave%20Buoy

Author contributions

GMR: conceptualization, investigation, methodology, visualisation, data curation, writing – original draft, writing – review & editing. **GRMB:** conceptualization, funding acquisition, methodology, investigation, supervision, data curation, writing – review & editing. **BLH:** investigation, writing – review & editing. **AJH:** investigation, writing – review & editing. **ZMS:** software, resources, writing – review & editing.

Competing interests

The authors declare that they have no conflict of interest.

Disclaimer

Copernicus Publications adds a standard disclaimer: "Copernicus Publications remains neutral with regard to jurisdictional claims made in the text, published maps, institutional affiliations, or any other geographical representation in this paper. While Copernicus Publications makes every effort to include appropriate place names, the final responsibility lies with the authors. Views expressed in the text are those of the authors and do not necessarily reflect the views of the publisher."
Please feel free to add disclaimer text at your choice, if applicable.

Acknowledgements

This research was supported by a grant from the Research Ireland Centre for Applied Geosciences (iCRAG). We thank William Hamilton (University of Galway) for assistance with drone survey and remote sensing data preparation, and Meredith Kelly, Josh Landis, and Peter Galloway (Dartmouth College) for providing the beryllium-9 carrier used in our measurements.

https://doi.org/10.5194/egusphere-2026-3761
Preprint. Discussion started: 15 September 2026

Financial support

This research was supported by a grant from the Research Ireland Centre for Applied Geosciences (iCRAG) under Grant Number 13/RC/2092_P2.

Review statement

The review statement will be added by Copernicus Publications listing the handling editor as well as all contributing referees according to their status anonymous or identified.

References

Agisoft LCC: Agisoft Metashape User Manual Professional Edition, Version 1.5, 2019.

Balco, G.: Production rate calculations for cosmic-ray-muon-produced 10Be and 26Al benchmarked against geological calibration data, Quaternary Geochronology, 39, 150–173, https://doi.org/10.1016/j.quageo.2017.02.001, 2017.

Balco, G., Stone, J. O., Lifton, N. A., and Dunai, T. J.: A complete and easily accessible means of calculating surface exposure ages or erosion rates from 10Be and 26Al measurements, Quaternary Geochronology, 3, 174–195, https://doi.org/https://doi.org/10.1016/j.quageo.2007.12.001, 2008.

Ballantyne, C. K., McCarroll, D., and Stone, J. O.: The Donegal ice dome, northwest Ireland: dimensions and chronology, J. Quaternary Sci., 22, 773–783, https://doi.org/10.1002/jqs.1116, 2007.

Best, J. L., Wignall, P. B., Best, J. L., Wignall, P. B., and International Association of Sedimentologists (Eds.): A field guide to the Carboniferous sediments of the Shannon Basin, Western Ireland, Wiley Blackwell, Chichester, West Sussex, 375 pp., 2016.

Bradley, S. L., Milne, G. A., Shennan, I., and Edwards, R.: An improved glacial isostatic adjustment model for the British Isles: GLACIAL ISOSTATIC ADJUSTMENT MODEL FOR THE BRITISH ISLES, J. Quaternary Sci., 26, 541–552, https://doi.org/10.1002/jqs.1481, 2011.

Braucher, R., Brown, E. T., Bourlès, D. L., and Colin, F.: In situ produced 10Be measurements at great depths: implications for production rates by fast muons, Earth and Planetary Science Letters, 211, 251–258, https://doi.org/10.1016/S0012-821X(03)00205-X, 2003.

Bromley, G., Bunce, C., Hall, B., Putnam, A., and McDermott, F.: Deglaciation of the Burren glacio-karst, western Ireland, during Termination 1: Implications for North Atlantic climate and karstification, J Quaternary Science, jqs.70068, https://doi.org/10.1002/jqs.70068, 2026.

Buchanan, D. H., Naylor, L. A., Hurst, M. D., and Stephenson, W. J.: Erosion of rocky shore platforms by block detachment from layered stratigraphy, Earth Surf Processes Landf, 45, 1028–1037, https://doi.org/10.1002/esp.4797, 2020.

Choi, K. H., Seong, Y. B., Jung, P. M., and Lee, S. Y.: Using Cosmogenic 10Be Dating to Unravel the Antiquity of a Rocky Shore Platform on the West Coast of Korea, Journal of Coastal Research, 28, 641, https://doi.org/10.2112/JCOASTRES-D-11-00087.1, 2012.

Clark, C. D., Ely, J. C., Hindmarsh, R. C. A., Bradley, S., Ignéczi, A., Fabel, D., Ó Cofaigh, C., Chiverrell, R. C., Scourse, J., Benetti, S., Bradwell, T., Evans, D. J. A., Roberts, D. H., Burke, M., Callard, S. L., Medialdea, A., Saher, M., Small, D., Smedley, R. K., Gasson, E., Gregoire, L., Gandy, N., Hughes, A. L. C., Ballantyne, C., Bateman, M. D., Bigg, G. R., Doole, J., Dove, D., Duller, G. A. T., Jenkins, G. T. H., Livingstone, S. L., McCarron, S., Moreton, S., Pollard, D., Praeg, D., Sejrup, H. P., Van Landeghem, K. J. J., and Wilson, P.: Growth and retreat of the last British–Irish Ice Sheet, 31 000 to 15 000 years ago: the BRITICE-CHRONO reconstruction, Boreas, 51, 699–758, https://doi.org/10.1111/bor.12594, 2022.

Clow, T., Willenbring, J. K., Young, A. P., Matsumoto, H., Hidy, A. J., and Shadrick, J. R.: Late Holocene Cliff Retreat in Del Mar, CA, Revealed From Shore Platform ^{10}Be Concentrations and Numerical Modeling, JGR Earth Surface, 128, e2022JF006855, https://doi.org/10.1029/2022JF006855, 2023.

Collinson, J. D., Martinsen, O., Bakken, B., and Kloster, A.: Early fill of the Western Irish Namurian Basin: a complex relationship between turbidites and deltas, Basin Research, 3, 223–242, https://doi.org/10.1111/j.1365-2117.1991.tb00131.x, 1991.

Colomina, I. and Molina, P.: Unmanned aerial systems for photogrammetry and remote sensing: A review, ISPRS Journal of Photogrammetry and Remote Sensing, 92, 79–97, https://doi.org/https://doi.org/10.1016/j.isprsjprs.2014.02.013, 2014.

Cooper, J. A. G., Jackson, D. W. T., Navas, F., McKenna, J., and Malvarez, G.: Identifying storm impacts on an embayed, high-energy coastline: examples from western Ireland, Marine Geology, 210, 261–280, https://doi.org/10.1016/j.margeo.2004.05.012, 2004.

Cosby, A. G., Lebakula, V., Smith, C. N., Wanik, D. W., Bergene, K., Rose, A. N., Swanson, D., and Bloom, D. E.: Accelerating growth of human coastal populations at the global and continent levels: 2000–2018, Scientific Reports, 14, 22489, https://doi.org/10.1038/s41598-024-73287-x, 2024.

Cox, R., Jahn, K. L., Watkins, O. G., and Cox, P.: Extraordinary boulder transport by storm waves (west of Ireland, winter 2013–2014), and criteria for analysing coastal boulder deposits, Earth-Science Reviews, 177, 623–636, https://doi.org/10.1016/j.earscirev.2017.12.014, 2018.

Cullen, N. D. and Bourke, M. C.: Clast abrasion of a rock shore platform on the Atlantic coast of Ireland: Clast abrasion of a rock shore platform, Earth Surf. Process. Landforms, 43, 2627–2641, https://doi.org/10.1002/esp.4421, 2018.

Davis, S. J., Guion, P. D., and Gutteridge, P.: Carboniferous Sedimentation and Volcanism on the Laurussian Margin, in: Geological history of Britain and Ireland, edited by: Woodcock, N. H. and Strachan, R. A., Wiley-Blackwell, Chichester, 233–273, 2012.

Devoy, R. J. N., Delaney, C., Carter, R. W. G., and Jennings, S. C.: Coastal Stratigraphies as Indicators of Environmental Changes upon European Atlantic Coasts in the Late Holocene, Journal of Coastal Research, 12, 564–588, 1996.

Dornbusch, U., Robinson, D. A., Moses, C., Williams, R., and Costa, S.: Retreat of Chalk cliffs in the eastern English Channel during the last century, Journal of Maps, 2, 71–78, https://doi.org/10.4113/jom.2006.46, 2006.

Dornbusch, U., Robinson, D. A., Moses, C. A., and Williams, R. B. G.: Temporal and spatial variations of chalk cliff retreat in East Sussex, 1873 to 2001, Marine Geology, 249, 271–282, https://doi.org/10.1016/j.margeo.2007.12.005, 2008.

Dunne, J., Elmore, D., and Muzikar, P.: Scaling factors for the rates of production of cosmogenic nuclides for geometric shielding and attenuation at depth on sloped surfaces, Geomorphology, 27, 3–11, https://doi.org/10.1016/S0169-555X(98)00086-5, 1999.

Flemming, N.: Form and Relation to Present Sea Level of Pleistocene Marine Erosion Features, The Journal of Geology, 73, https://doi.org/10.1086/627116, 1965.

Furlani, S. and Cucchi, F.: Downwearing rates of vertical limestone surfaces in the intertidal zone (Gulf of Trieste, Italy), Marine Geology, 343, 92–98, https://doi.org/10.1016/j.margeo.2013.06.005, 2013.

Gallagher, S., Tiron, R., and Dias, F.: A Detailed Investigation of the Nearshore Wave Climate and the Nearshore Wave Energy Resource on the West Coast of Ireland, in: Volume 8: Ocean Renewable Energy, ASME 2013 32nd International Conference on Ocean, Offshore and Arctic Engineering, Nantes, France, V008T09A046, https://doi.org/10.1115/OMAE2013-10719, 2013.

Gallagher, S., Tiron, R., and Dias, F.: A long-term nearshore wave hindcast for Ireland: Atlantic and Irish Sea coasts (1979–2012): Present wave climate and energy resource assessment, Ocean Dynamics, 64, 1163–1180, https://doi.org/10.1007/s10236-014-0728-3, 2014.

https://doi.org/10.5194/egusphere-2026-3761
Preprint. Discussion started: 15 September 2026

Gómez-Pazo, A., Pérez-Alberti, A., and Trenhaile, A.: Tracking the behavior of rocky coastal cliffs in northwestern Spain, Environ Earth Sci, 80, 757, https://doi.org/10.1007/s12665-021-09929-4, 2021.

Gosse, J. C. and Phillips, F. M.: Terrestrial in situ cosmogenic nuclides: theory and application, Quaternary Science Reviews, 20, 1475–1560, https://doi.org/https://doi.org/10.1016/S0277-3791(00)00171-2, 2001.

Graham, J. R., Ní Bhroin, C., and Sevastopulo, G. D.: The Carboniferous geology of northern Donegal Bay, Irish Journal of Earth Sciences, 32, 29, https://doi.org/10.3318/ijes.2014.32.29, 2014.

Hurst, M. D., Rood, D. H., Ellis, M. A., Anderson, R. S., and Dornbusch, U.: Recent acceleration in coastal cliff retreat rates on the south coast of Great Britain, Proc. Natl. Acad. Sci. U.S.A., 113, 13336–13341, https://doi.org/10.1073/pnas.1613044113, 2016.

Hurst, M. D., Rood, D. H., and Ellis, M. A.: Controls on the distribution of cosmogenic ¹⁰Be across shore platforms, Earth Surf. Dynam., 5, 67–84, https://doi.org/10.5194/esurf-5-67-2017, 2017.

Jeong, A., Seong, Y. B., Choi, K. H., Swirad, Z. M., Lee, C.-H., and Yu, B. Y.: Shore platform erosion and cliff retreat in the Eastern Korea: A quantified assessment using 10Be concentrations and numerical modeling, Marine Geology, 472, 107291, https://doi.org/10.1016/j.margeo.2024.107291, 2024.

Jeong, A., Seong, Y. B., Choi, K. H., and Swirad, Z. M.: Global patterns of shore platform evolution and cliff retreat: Insights from cosmogenic radionuclides, Earth-Science Reviews, 272, 105323, https://doi.org/10.1016/j.earscirev.2025.105323, 2026.

Kennedy, A. B., Cox, R., and Dias, F.: Storm Waves May Be the Source of Some “Tsunami” Coastal Boulder Deposits, Geophysical Research Letters, 48, https://doi.org/10.1029/2020gl090775, 2021.

Kennedy, D. M., Stephenson, W. J., and Naylor, L. A.: Chapter 1 Introduction to the rock coasts of the world, Memoirs, 40, 1–5, https://doi.org/10.1144/m40.1, 2014.

Knight, J. and Burningham, H.: Boulder dynamics on an Atlantic-facing rock coastline, northwest Ireland, Marine Geology, 283, 56–65, https://doi.org/10.1016/j.margeo.2010.07.008, 2011.

Kohl, C. P. and Nishiizumi, K.: Chemical isolation of quartz for measurement of in-situ -produced cosmogenic nuclides, Geochimica et Cosmochimica Acta, 56, 3583–3587, https://doi.org/10.1016/0016-7037(92)90401-4, 1992.

Kuchar, J., Milne, G., Hubbard, A., Patton, H., Bradley, S., Shennan, I., and Edwards, R.: Evaluation of a numerical model of the British–Irish ice sheet using relative sea-level data: implications for the interpretation of trimline observations, J Quaternary Science, 27, 597–605, https://doi.org/10.1002/jqs.2552, 2012.

Lal, D.: Cosmic ray labeling of erosion surfaces: in situ nuclide production rates and erosion models, Earth and Planetary Science Letters, 104, 424–439, https://doi.org/10.1016/0012-821X(91)90220-C, 1991.

Lifton, N., Sato, T., and Dunai, T. J.: Scaling *in situ* cosmogenic nuclide production rates using analytical approximations to atmospheric cosmic-ray fluxes, Earth and Planetary Science Letters, 386, 149–160, https://doi.org/10.1016/j.epsl.2013.10.052, 2014.

Lozano, I., Devoy, R. J. N., May, W., and Andersen, U.: Storminess and vulnerability along the Atlantic coastlines of Europe: analysis of storm records and of a greenhouse gases induced climate scenario, Marine Geology, 210, 205–225, https://doi.org/10.1016/j.margeo.2004.05.026, 2004.

DigitalOcean.ie: https://www.digitalocean.ie/, last access: 23 July 2025.

Home | DigitalOcean.ie: https://www.digitalocean.ie/, last access: 23 July 2025.

Minogue, R., Foley, K., Collins, T., Hennessy, R., Doherty, P., Vaughan, E., and Black, D.: Definition and classification of Ireland's seascapes, 2020.

Nauton-Fourteu, M., Tyrrell, S., Morton, A., Mark, C., O'Sullivan, G. J., and Chew, D. M.: Constraining recycled detritus in quartz-rich sandstones: Insights from a multi-proxy provenance study of the Mid-Carboniferous, Clare Basin, western Ireland, Basin Research, 33, 342–363, https://doi.org/10.1111/bre.12469, 2020.

Nishiizumi, K., Imamura, M., Caffee, M. W., Southon, J. R., Finkel, R. C., and McAninch, J.: Absolute calibration of 10Be AMS standards, Nuclear Instruments and Methods in Physics Research Section B: Beam Interactions with Materials and Atoms, 258, 403–413, https://doi.org/10.1016/j.nimb.2007.01.297, 2007.

O'Brien, L., Renzi, E., Dudley, J. M., Clancy, C., and Dias, F.: Catalogue of extreme wave events in Ireland: revised and updated for 14 680 BP to 2017, Nat. Hazards Earth Syst. Sci., 18, 729–758, https://doi.org/10.5194/nhess-18-729-2018, 2018.

Ochs, M. and Ivy-Ochs, S.: The chemical behavior of Be, Al, Fe, Ca and Mg during AMS target preparation from terrestrial silicates modeled with chemical speciation calculations, Nuclear Instruments and Methods in Physics Research Section B: Beam Interactions with Materials and Atoms, 123, 235–240, https://doi.org/10.1016/S0168-583X(96)00680-5, 1997.

Paris, R., Naylor, L. A., and Stephenson, W. J.: Boulders as a signature of storms on rock coasts, Marine Geology, 283, 1–11, https://doi.org/10.1016/j.margeo.2011.03.016, 2011.

Peel, M. C., Finlayson, B. L., and McMahon, T. A.: Updated world map of the Köppen-Geiger climate classification, Hydrol. Earth Syst. Sci., 11, 1633–1644, https://doi.org/10.5194/hess-11-1633-2007, 2007.

Pereira, D.: Wind Rose, 2025.

https://doi.org/10.5194/egusphere-2026-3761
Preprint. Discussion started: 15 September 2026

Pointon, M. A., Cliff, R. A., and Chew, D. M.: The provenance of Western Irish Namurian Basin sedimentary strata inferred using detrital zircon U-Pb LA-ICP-MS geochronology: PROVENANCE OF WESTERN IRISH NAMURIAN BASIN STRATA, Geol. J., 47, 77–98, https://doi.org/10.1002/gj.1335, 2012.

Prémaillon, M., Regard, V., Dewez, T. J. B., and Auda, Y.: GlobR2C2 (Global Recession Rates of Coastal Cliffs): a global relational database to investigate coastal rocky cliff erosion rate variations, Earth Surf. Dynam., 6, 651–668, https://doi.org/10.5194/esurf-6-651-2018, 2018.

Putnam, A. E., Bromley, G. R. M., Rademaker, K., and Schaefer, J. M.: In situ 10Be production-rate calibration from a 14C-dated late-glacial moraine belt in Rannoch Moor, central Scottish Highlands, Quaternary Geochronology, 50, 109–125, https://doi.org/10.1016/j.quageo.2018.11.006, 2019.

Regard, V., Dewez, T., Bourlès, D. L., Anderson, R. S., Duperret, A., Costa, S., Leanni, L., Lasseur, E., Pedoja, K., and Maillet, G. M.: Late Holocene seacliff retreat recorded by 10Be profiles across a coastal platform: Theory and example from the English Channel, Quaternary Geochronology, 11, 87–97, https://doi.org/https://doi.org/10.1016/j.quageo.2012.02.027, 2012.

Rink, G. and Bromley, G.: A coupled cosmogenic-modelling approach to quantifying Holocene erosion of Ireland's hard-rock coastal cliffs (v1), https://doi.org/10.5281/ZENODO.20844617, 2026.

Rink, G. M., Farrell, E. J., and Bromley, G. R. M.: Quantifying Aperiodic Cliff Top and Cliff Face Retreat Rates for an Eroding Drumlin on Ireland's Atlantic Coast Using Structure-from-Motion, Geosciences, 14, 165, https://doi.org/10.3390/geosciences14060165, 2024.

Rogers, H. E., Swanson, T. W., and Stone, J. O.: Long-term shoreline retreat rates on Whidbey Island, Washington, USA, Quat. res., 78, 315–322, https://doi.org/10.1016/j.yqres.2012.06.001, 2012.

Ruggiero, P., Kratzmann, M. G., Himmelstoss, E. A., Reid, D., Allan, J., and Kaminsky, G.: National Assessment of Shoreline Change: Historical Shoreline Change Along the Pacific Northwest Coast, U.S. Geological Survey, 2013.

Schwanghart, W. and Kuhn, N. J.: TopoToolbox: A set of Matlab functions for topographic analysis, Environmental Modelling & Software, 25, 770–781, https://doi.org/10.1016/j.envsoft.2009.12.002, 2010.

Schwanghart, W. and Scherler, D.: Short Communication: TopoToolbox 2 – MATLAB-based software for topographic analysis and modeling in Earth surface sciences, Earth Surf. Dynam., 2, 1–7, https://doi.org/10.5194/esurf-2-1-2014, 2014.

Shadrick, J. R., Hurst, M. D., Piggott, M. D., Hebditch, B. G., Seal, A. J., Wilcken, K. M., and Rood, D. H.: Multi-objective optimisation of a rock coast evolution model with cosmogenic \chem^10Be analysis for the

https://doi.org/10.5194/egusphere-2026-3761
Preprint. Discussion started: 15 September 2026

quantification of long-term cliff retreat rates, Earth Surface Dynamics, 9, 1505–1529, https://doi.org/10.5194/esurf-9-1505-2021, 2021.

Shadrick, J. R., Rood, D. H., Hurst, M. D., Piggott, M. D., Hebditch, B. G., Seal, A. J., and Wilcken, K. M.: Sea-level rise will likely accelerate rock coast cliff retreat rates, Nat Commun, 13, 7005, https://doi.org/10.1038/s41467-022-34386-3, 2022.

Shadrick, J. R., Rood, D. H., Hurst, M. D., Piggott, M. D., Wilcken, K. M., and Seal, A. J.: Constraints on long-term cliff retreat and intertidal weathering at weak rock coasts using cosmogenic ^{10}Be, nearshore topography and numerical modelling, Earth Surf. Dynam., 11, 429–450, https://doi.org/10.5194/esurf-11-429-2023, 2023.

Shaw, J. and Carter, R. W. G.: Coastal peats from northwest Ireland: implications for late-Holocene relative sea-level change and shoreline evolution, Boreas, 23, 74–91, https://doi.org/10.1111/j.1502-3885.1994.tb00588.x, 1994.

Shennan, I., Bradley, S. L., and Edwards, R.: Relative sea-level changes and crustal movements in Britain and Ireland since the Last Glacial Maximum, Quaternary Science Reviews, 188, 143–159, https://doi.org/10.1016/j.quascirev.2018.03.031, 2018.

Smith, A. G. and Pilcher, J. R.: Radiocarbon Dates and Vegetational History of the British Isles, The New Phytologist, 72, 903–914, 1973.

Stephenson, W. J.: Shore platforms: a neglected coastal feature?, Progress in Physical Geography: Earth and Environment, 24, 311–327, https://doi.org/10.1177/030913330002400301, 2000.

Stephenson, W. J., Kirk, R. M., Hemmingsen, S. A., and Hemmingsen, M. A.: Decadal scale micro erosion rates on shore platforms, Geomorphology, 114, 22–29, https://doi.org/10.1016/j.geomorph.2008.10.013, 2010.

Stone, J.: A Rapid Fusion Method for Separation of Beryllium-10 From Soils and Silicates, Geochimica et Cosmochimica Acta, 62, 555–561, https://doi.org/10.1016/S0016-7037(97)00340-2, 1998.

Stone, J. O.: Air pressure and cosmogenic isotope production, J. Geophys. Res., 105, 23753–23759, https://doi.org/10.1029/2000JB900181, 2000.

Strunden, J., Ehlers, T. A., Brehm, D., and Nettesheim, M.: Spatial and temporal variations in rockfall determined from TLS measurements in a deglaciated valley, Switzerland: ROCKFALL IN A DEGLACIATED VALLEY, J. Geophys. Res. Earth Surf., 120, 1251–1273, https://doi.org/10.1002/2014JF003274, 2015.

Sunamura, T.: Geomorphology of rocky coasts, Wiley, 1992.

Swirad, Z. M.: zswirad/RockCoast10Be: 2.0, , https://doi.org/10.5281/ZENODO.15783544, 2025.

Swirad, Z. M. and Young, A. P.: Spatial and temporal trends in California coastal cliff retreat, Geomorphology, 412, 108318, https://doi.org/10.1016/j.geomorph.2022.108318, 2022.

https://doi.org/10.5194/egusphere-2026-3761
Preprint. Discussion started: 15 September 2026

Swirad, Z. M., Rosser, N. J., and Brain, M. J.: Identifying mechanisms of shore platform erosion using Structure-from-Motion (SfM) photogrammetry, Earth Surf. Process. Landforms, 44, 1542–1558, https://doi.org/10.1002/esp.4591, 2019.

Swirad, Z. M., Rosser, N. J., Brain, M. J., Rood, D. H., Hurst, M. D., Wilcken, K. M., and Barlow, J.: Cosmogenic exposure dating reveals limited long-term variability in erosion of a rocky coastline, Nat Commun, 11, 3804, https://doi.org/10.1038/s41467-020-17611-9, 2020.

Tiron, R., Gallagher, S., Gleeson, E., Dias, F., and McGrath, R.: The Future Wave Climate of Ireland: From Averages to Extremes, Procedia IUTAM, 17, 40–46, https://doi.org/10.1016/j.piutam.2015.06.007, 2015.

Trenhaile, A. S.: The Geometry of Shore Platforms in England and Wales, Transactions of the Institute of British Geographers, 129, https://doi.org/10.2307/621519, 1974.

Trenhaile, A. S.: Modeling the development of wave-cut shore platforms, Marine Geology, 166, 163–178, https://doi.org/10.1016/S0025-3227(00)00013-X, 2000.

Trenhaile, A. S.: Modeling the role of weathering in shore platform development, Geomorphology, 94, 24–39, https://doi.org/10.1016/j.geomorph.2007.04.002, 2008.

Trenhaile, A. S. and Porter, N. J.: Shore platform downwearing in eastern Canada; A 9–14 year micro-erosion meter record, Geomorphology, 311, 90–102, https://doi.org/10.1016/j.geomorph.2018.03.024, 2018.

Van Blunk, A., Kennedy, A. B., and Cox, R.: Interplay Between Coastal Elevation and Wave Height Controls the Occurrence of Coastal Boulder Deposits in the Aran Islands, Ireland, Front. Earth Sci., 9, https://doi.org/10.3389/feart.2021.715383, 2021.

Walsh, S.: A summary of climate averages for Ireland, 1981-2010, Met Éireann, 2012.

Westoby, M. J., Brasington, J., Glasser, N. F., Hambrey, M. J., and Reynolds, J. M.: ‘Structure-from-Motion’ photogrammetry: A low-cost, effective tool for geoscience applications, Geomorphology, 179, 300–314, https://doi.org/https://doi.org/10.1016/j.geomorph.2012.08.021, 2012.

Whitmore, R. J., Norton, K. P., Ashworth, L., and Mackintosh, A. N.: Sequential quartz purification of 125–63 µm material for in-situ cosmogenic nuclide analysis, Nuclear Instruments and Methods in Physics Research Section B: Beam Interactions with Materials and Atoms, 511, 105–112, https://doi.org/10.1016/j.nimb.2021.11.011, 2022.

Williams, J. G., Rosser, N. J., Hardy, R. J., and Brain, M. J.: The Importance of Monitoring Interval for Rockfall Magnitude-Frequency Estimation, J. Geophys. Res. Earth Surf., 124, 2841–2853, https://doi.org/10.1029/2019JF005225, 2019.

Young, A. P. and Carilli, J. E.: Global distribution of coastal cliffs, Earth Surf Processes Landf, 44, 1309–1316, https://doi.org/10.1002/esp.4574, 2019.

https://doi.org/10.5194/egusphere-2026-3761
Preprint. Discussion started: 15 September 2026

Young, A. P., Guza, R. T., Matsumoto, H., Merrifield, M. A., O'Reilly, W. C., and Swirad, Z. M.: Three years of weekly observations of coastal cliff erosion by waves and rainfall, Geomorphology, 375, 107545, https://doi.org/10.1016/j.geomorph.2020.107545, 2021.